U.S.NRC
United States Nuclear Regulatory Commission
Protecting People and the Environment

RIL 2025-xx

Follow-up Paleoliquefaction Studies of the Central Virginia Seismic Zone

Date Published: XXXX 2025

Prepared by:

M. P. Tuttle, M. Tuttle & Associates
P.O. Box 345, Georgetown, ME 04548

K. Dyer-Williams, VanLeen Associates
P.O. Box 156, Columbia, MD 21045

S. L. Forman, Department of Geosciences
Baylor University, Waco, TX 76798

K. Tucker, PangaeaGIS
2065 Leichester Lane, Memphis, TN 38134

Carlos Velez, M. Tuttle & Associates
P.O. Box 345, Georgetown, ME 04548

Research Information Letter
Office of Nuclear Regulatory Research

DISCLAIMER

ABSTRACT

Recently discovered sand dikes, sills, diapirs, and injected krotovinas along the Appomattox River west of Richmond, VA, and a dike, pseudonodules, diapirs, and flames along the Rapidan River west of Fredericksburg, VA, are interpreted as earthquake-induced liquefaction features. The features were found during river surveys that extend the search area for liquefaction features in an effort to better understand the earthquake potential of the Central Virginia seismic zone (CVSZ) following the 2011, moment magnitude, **M**, 5.7 ± 0.1 Mineral, Virginia, earthquake.

Along the Appomattox, there are at least two generations of the features. The older generation is very weathered and characterized by bioturbation and mottling; whereas, the younger generation is relatively unweathered and crosscuts older features. For most of the weathered liquefaction features on the Appomattox River, as well as other features previously found across the region, dating is limited to maximum constraining ages. However, dating at a newly found site on the Appomattox River provides both minimum and maximum constraining ages. These ages, combined with the youngest maximum constraining ages for weathered features along the Mattaponi and Pamunkey rivers, suggest that many of the features formed ca. 2,640 ± 80 yr B.P. Given an apparent lack of crosscutting relationships, older, weathered features along rivers in the region may have formed during the same earthquake, though earlier events cannot be ruled out. Reevaluating scenario earthquakes using liquefaction potential analysis, the broader distribution of weathered features, including the Appomattox, could be the result of one moment magnitude, **M**, 6.5-6.75 earthquake located near Holly Grove, Macon, or Wyndham Forest, VA. Considering size distribution of dikes, specifically average dike widths for different river segments, suggests the event may have been located closest to Wyndham Forest, northwest of Richmond. Alternatively, the weathered features may have formed during three **M** 6.25-6.5 earthquakes centered near Mineral, Holly Grove, and Ashland, though there is no unequivocal evidence to support multiple large earthquakes during the Holocene and Late Pleistocene (0-0.0117 million years ago, or Ma, and 0.0117-0.129 Ma, respectively; Cohen et al., 2022).

The finding of young liquefaction features along the Appomattox River, in additional to young features previously found on the James and Pamunkey rivers, also broadens the area of historical liquefaction towards the south. According to liquefaction potential analysis, a combination of the historical earthquakes of 1758, 1774, and 1875 C.E. could account for the formation of the young features on all three rivers if the events were in the **M** 5.25-5.5 range.

Dating of liquefaction features along the Rapidan River provides minimum and maximum constraining ages and suggests that the features formed ca. 1690 ± 50 yr C.E. No earthquake is known to have occurred in the CVSZ during this period, but the description of “terre tremblante” on a map published in 1718 indicates that early colonists experienced earthquakes in the Rapidan area. Liquefaction potential analysis suggests that an earthquake of **M** 5.5-5.75 produced by a local source, within 10 km, could induce liquefaction along the Rapidan River.

FOREWORD

The U.S. Nuclear Regulatory Commission (NRC) requires an evaluation to determine the Safe Shutdown Earthquake (SSE) ground motion for a nuclear power plant site as specified in 10 CFR Part 100. A performance-based approach to define site-specific earthquake ground motion is one component in the development and evaluation of the SSE. Regulatory Guide 1.208 provides guidance on this performance-based approach which implements a probabilistic seismic hazard analysis. The probabilistic seismic hazard analysis is dependent on the characterization of seismic (earthquake) sources, with the key parameters in characterizing seismic sources being their location, timing, and size. The historical record of measured earthquakes is limited; therefore, the study of prehistoric earthquakes is extremely valuable in characterizing seismic sources. The study of prehistoric liquefaction features, paleoliquefaction, is one method used to characterize seismic sources.

Regulatory Guide 1.208, A Performance-Based Approach to Define the Site-Specific Earthquake Ground Motion, and the Standard Review Plan for the Review of Safety Analysis Reports for Nuclear Power Plants: LWR Edition (NUREG-0800), Section 2.5.1, provides guidance to license applicants and NRC staff, respectively, on the review of seismic sources. This document provides results of a follow-up studies that provides additional information relevant to the approximate timing, locations, and magnitudes of past earthquakes in the Central Virginia seismic zone (CVSZ) and surrounding region, key parameters for the assessment of earthquake hazard in the Mid-Atlantic region and Greater Washington D.C. area.

TABLE OF CONTENTS

LIST OF FIGURES

LIST OF TABLES

ACKNOWLEDGMENTS

This research project is sponsored by the U.S. NRC under contract 31310023C0012. The views and conclusions contained in the document are those of the authors and should not be interpreted as necessarily representing the official policies of the U.S. Government. Martitia Tuttle and Carlos Velez conducted river surveys and revisited selected liquefaction sites to collect samples for dating purposes. Kathleen Dyer-Williams performed liquefaction analysis for scenario earthquakes and tabulated results for the report. Steve Forman oversaw optically-stimulated luminescence (OSL) dating at Geoluminescence Dating Research Lab at Baylor University, recalculated OSL ages as methodology improved over the course of the project, and contributed to the dating of liquefaction features. Kathleen Tucker maintained the liquefaction database and generated figures within a GIS framework. Previously, Carl Benson and Ramesh Neupane of the Virginia Department of Transportation provided access to geotechnical data for the project and additional data was downloaded during this study. Radiocarbon and optically-stimulated luminescence dating were performed by Beta Analytic, Inc. and Geoluminescence Dating Research Lab at Baylor University, respectively. Many thanks to property owners who gave access to the rivers. Mark Carter, a collaborator during our previous liquefaction studies in the CVSZ, provided information about the regional geology and his findings of liquefaction features along the Nottoway and South Anna rivers. Many thanks to Rasool Anooshehpoor and Thomas Weaver of the NRC who provided valuable guidance and support during the contract. Thomas Weaver also reviewed this report and provided helpful comments and suggestions.

1 INTRODUCTION

The August 23, 2011, moment magnitude, **M**, 5.7 ± 0.1 earthquake struck ~130 km southwest of Washington, D.C. in the Mid-Atlantic region (Figure 1-1; Horton et al., 2015). The moderate earthquake occurred in the Central Virginia seismic zone (CVSZ), an area of diffuse seismicity, with most earthquakes occurring within ~60 km of the James River between Richmond and Charlottesville (Chapman, 2013 and 2015). The 2011 Mineral earthquake induced localized liquefaction in alluvial deposits of the South Anna River and damaged residences, buildings, schools, and earthen dams in the epicentral area (Green et al., 2015), as well as bridges, prominent buildings, and monuments in Washington, D.C. (Horton et al., 2015). The Mineral event is the largest earthquake to have occurred in the CVSZ during the historical period and raised concerns about the earthquake potential of the seismic zone, leading to investigations of the paleoearthquake history of the region.

During a paleoliquefaction study following the 2011 Mineral earthquake, more than forty liquefaction features, primarily sand dikes (0.5-20 cm wide) and several soft-sediment deformation structures, were found along the Mattaponi and Pamunkey rivers in the Coastal Plain east of the Fall Line (the boundary between Coastal Plain sedimentary rocks to the east and Piedmont crystalline rocks to the west) as well as along the James and South Anna rivers, and Stigger Creek, a tributary to the Rivanna River, in the Appalachian Piedmont (Figure 1-1; Tuttle et al., 2021). On the basis of radiocarbon (^{14}C) dating and weathering characteristics, the liquefaction features were attributed to at least two earthquakes during the Late Holocene. The younger features are relatively small, few in number, occur on the James and Pamunkey rivers, and formed since 280 yr B.P. (before 1950 C.E.). One or more of the historical earthquakes of 1758, 1774, and 1875 C.E. were likely responsible for these features if they were in the **M** 5-5.75 range and located within close proximity to the features. The older features are larger, more numerous, and more broadly distributed than the younger features. Ages of many of the older features are poorly constrained, but some of the features clearly formed between 280 and 2730 years ago. Given the absence of crosscutting relationships and no significant differences in their weathering characteristics, the older features were interpreted to have formed during the same event, though earlier events could not be ruled out. Evaluation of scenario earthquakes indicated that the regional distribution of the older liquefaction features could be explained by one event of **M** 6.25-6.5 located near Holly Grove, or **M** 6.75 earthquake near Ashland or Mineral; alternatively, they could be explained by two events, one of **M** 6.0 near Mineral and a second of **M** 6.25 near Ashland.

Recently, during NRC contract #31310019C0028 entitled, "Paleoliquefaction studies in the CVSZ," two generations of liquefaction features, including sand dikes and intruded krotivina, were found along the Appomattox River (Tuttle et al., 2023a). The older features are bioturbated and mottled; whereas, the younger features are unweathered and crosscut the older features. On the basis of optically-stimulated luminescence (OSL) dating of host sediment, the older features were estimated to have formed ca. 3 thousand years ago (ka) ± 500 yr. The relatively unweathered, younger features were thought to be historical in age. The finding of two generations of features along the Appomattox is similar to previous findings along other rivers in the CVSZ (Tuttle et al., 2021). In addition, dating of paleoliquefaction features along the Appomattox helped to narrow the age estimate of the paleoearthquake that caused liquefaction across the CVSZ.

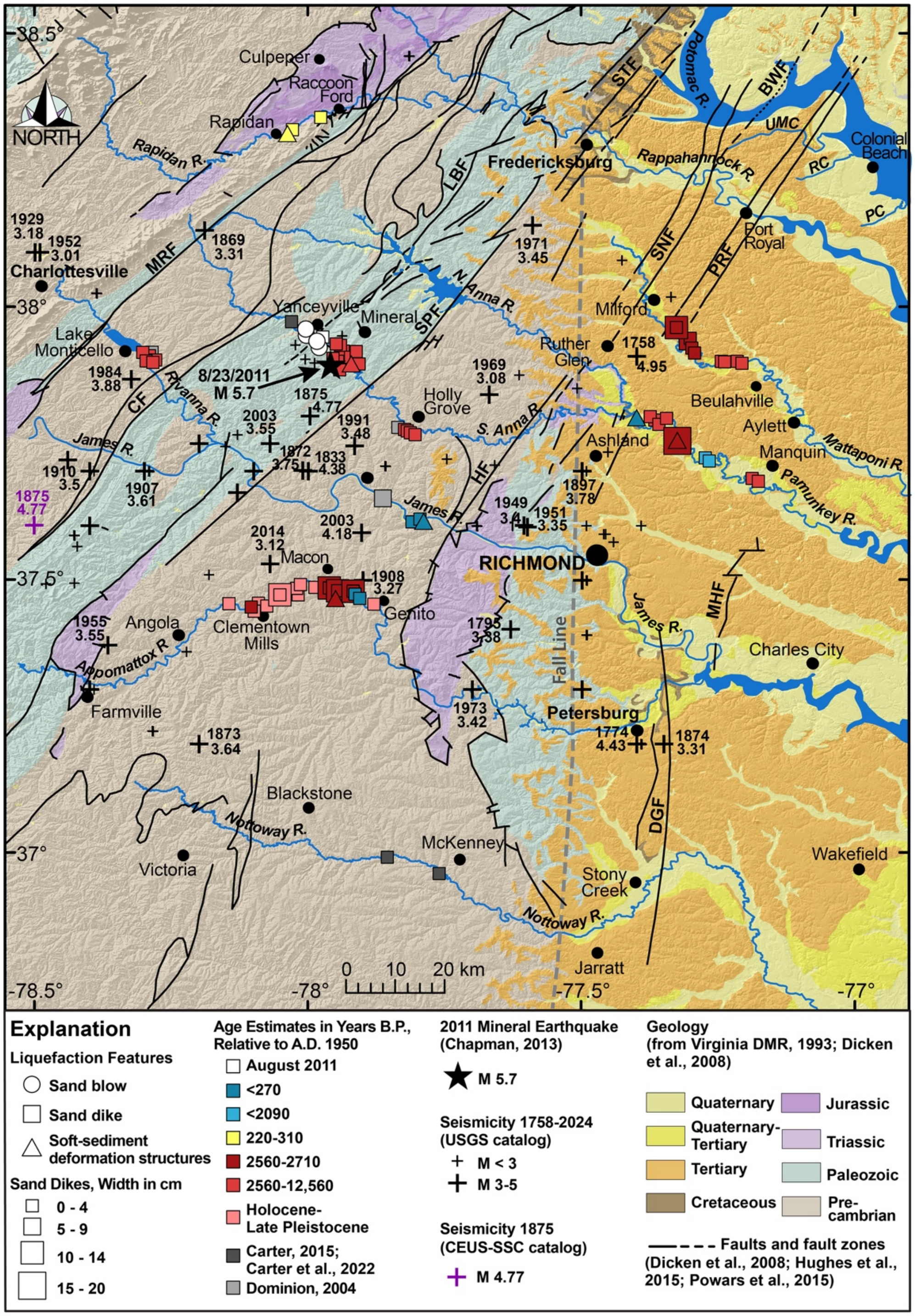

Figure 1-1: Map showing 2011, M 5.7, Mineral earthquake and other earthquakes in CVSZ, liquefaction features that formed during 2011 mainshock, and liquefaction features found during pre- and post-2011 studies. During this study, additional surveys for and/or study of liquefaction features were conducted along portions of the Appomattox, Nottoway, Rapidan, and Rivanna (Stigger Creek) rivers. Faults and fault zones: CF=Chopawamsic; LBF=Long Branch; MRF=Mountain Run; SPF=Spotsylvania; HF=Hylas; SNF=Skinkers Neck; PRF= Port Royal; DGF=Dutch Gap; and MHF=Malvern Hill.

Also during the NRC contract #31310019C0028, soft-sediment deformation structures (SSDs), including pseudonodules and flames, and a small sand dike were found on the Rapidan River north of Mineral and west of Fredericksburg (Figure 1-1; Tuttle et al., 2023). ^{14}C dating at one of the sites indicated that the possible liquefaction features formed between 60-1830 yr B.P. It was recommended to search for additional liquefaction features along the Rapidan and to improve the age estimate of the features.

During a separate study involving geological mapping south of the Appomattox River and west of the Fall Line, several sand dikes were found on the Nottoway River (Figure 1-1; Carter et al., 2020, 2022). Initial dating of the features suggested that they formed between 4-9 ka. This timing predates the ~3 ka ± 500 yr paleoearthquake, suggesting the possibility of an earlier event during the Holocene at least in the Nottoway area.

The recent discoveries of likely earthquake-induced liquefaction features along the Appomattox and Nottoway rivers and possible liquefaction features along the Rapidan River have implications for earthquake potential of the CVSZ and Mid-Atlantic region (Tuttle et al., 2023a). This study follows up on these recent findings and aims to determine if additional liquefaction features occur along these three rivers, to improve age estimates of liquefaction features, and to further reduce uncertainties related to the timing, source areas, magnitudes, and recurrence of large earthquakes during the past 10 kyr (thousand years).

2 PALEOLIQUEFACTION STUDIES AND SEISMIC HAZARD ASSESSMENT

Paleoliquefaction studies have helped to assess the earthquake potential of seismic zones in Central and Eastern United States (CEUS) and Southeastern Canada (see Tuttle and Hartleb, 2012, for a review of regional paleoliquefaction studies) and have contributed to the national seismic hazard model (NSHM). As the result of the 2011 Mineral earthquake and subsequent seismological and geological studies, the CVSZ was recognized as a significant earthquake source and added to the 2023 NSHM (Petersen et al., 2024). Subsequent studies identified a likely source area for the Mineral earthquake 6-8 km below the surface (Chapman, 2013) and a blind reverse fault named the Quail fault as the possible source (Horton et al., 2015). Geomorphic features associated with this fault include deformation and uplift of river terraces and changes in sinuosity of the South Anna River (Berti et al., 2015; Pazzaglia et al., 2021). Liquefaction features found in the CVSZ were interpreted to record one or two historical earthquakes in the **M** 5-5.75 range and one or two paleoearthquakes in the **M** 6-6.75 range, with preference given to one **M** 6.25-6.5 event near Holly Grove (Tuttle et al., 2021).

In the 2023 NSHM, the CVSZ source is represented by two fault-zone polygons: a small (local) polygon based on the location of the Mineral earthquake and the deformed river terraces in the vicinity of the earthquake and a large (regional) polygon based on paleoliquefaction features (Shumway et al., 2024; Figure 2-1). The CVSZ is modeled as a fault-plane polygon, rather than a fault section, because of the lack of evidence of fault rupture during the Mineral earthquake or previous earthquakes. Using a new magnitude-area relationship (Shaw, 2023), **M**max was determined for average, low, and high values based on the lengths of the northeast axes of the two polygons and a 15 km depth of rupture (Shumway et al., 2024). An upper limit of **M** 6.5 was placed on the magnitude distribution based on paleoliquefaction data available at the time (Tuttle et al., 2021). A recurrence interval range of 429-7692 for a large earthquake was also drawn from paleoliquefaction data and used to calculate a 5-point rate and weight distribution. The CVSZ source was assigned 50% weight to reflect uncertainty regarding whether or not it represents a unique source relative to background gridded seismicity sources (Shumway et al., 2024). Additional paleoliquefaction data collected since 2021 during NRC contract #31310019C0028 and this study are likely to lead to revisions of the regional fault-zone polygon as well as estimates of **M**max and recurrence times of repeating large-magnitude earthquakes (RLMEs).

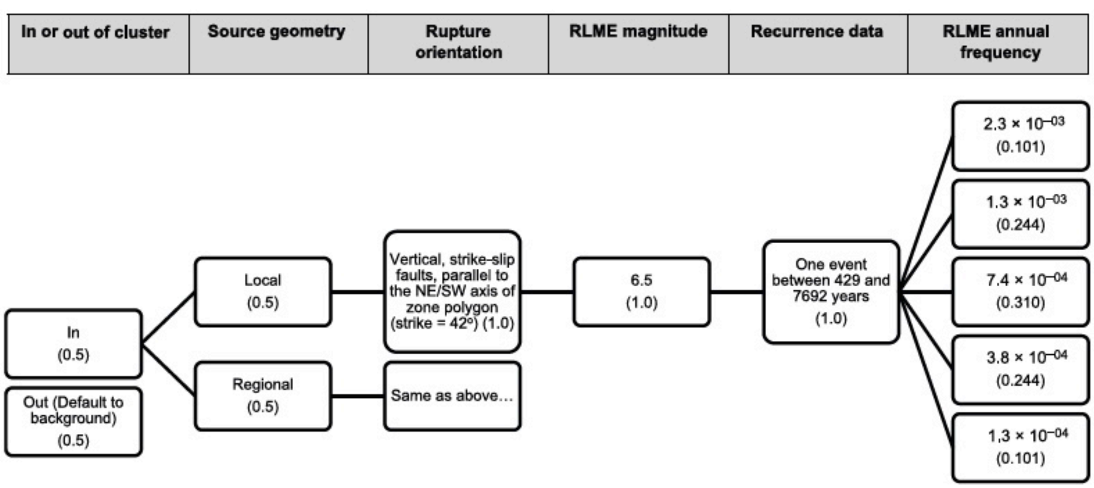

Figure 2-1: Logic tree of the central Virginia fault-zone polygon source (from Shumway et al., 2024). Source geometry from Thompson Jobe et al. (2022) based on Pazzaglia et al. (2021) and Tuttle et al. (2021).

3 PROJECT METHODS AND TASKS

This paleoliquefaction study employs best practices described in NUREG/CR-7238 guidance document (Tuttle et al., 2018) and *Geosciences* review article (Tuttle et al., 2019). As discussed in these two documents, accurate identification of liquefaction features is of utmost importance. In this study, as in the prior CVSZ investigation (Tuttle et al., 2021), possible earthquake-induced liquefaction features are carefully examined and evaluated using diagnostic criteria developed from studies of liquefaction features that formed during modern and historical earthquakes. Confidence values are assigned to possible liquefaction features found during this and the previous study, and those features in which there is high or medium confidence are used to interpret likely source areas of causative earthquake.

Estimating the timing of past earthquakes is based on dating of liquefaction features. Therefore, samples for ^{14}C and OSL dating are collected from sediment in which liquefaction features occur to try to constrain the age estimates of liquefaction features as narrowly as possible. Age estimates of liquefaction features help to correlate features across the region. The distribution and size of liquefaction features combined with evaluations of scenario earthquakes are used to interpret likely locations and magnitudes of the earthquakes that induced liquefaction. Scenario earthquakes for new hypothetical sources, as well as those previously considered (Tuttle et al., 2021), are evaluated by comparing predicted liquefaction with observed liquefaction. The various tasks undertaken and methods employed during this study are described in more detail below.

3.1 <u>River Surveys</u>

Reconnaissance for earthquake-induced liquefaction features was conducted along selected portions of the Appomattox, Nottoway, and Rapidan Rivers. Along the Appomattox River, surveys were conducted along segments upstream and downstream from the previously found features near Macon (Figures 1-1 and 3-1). Along the Nottoway River, surveys were conducted along segments near Jarratt and Stony Creek, downriver from liquefaction sites previously found by Carter et al. (2022). A portion of the Rapidan River was resurveyed and two possible liquefaction sites revisited to collect additional samples for dating. Also, a liquefaction site on Stigger Creek, close to its confluence with the Rivanna River, was revisited and additional samples collected to try to better constrain the age estimate of liquefaction features there.

The rivers surveys were conducted in October 2023 when river levels were low and cutbanks well exposed. The surveys were conducted by canoe and, in the case of Stigger Creek, on foot. River cutbanks were closely examined and locations of earthquake-induced liquefaction features were measured with a hand-held global positioning system receiver and marked on topographic maps. Information about the study sites, geologic setting, and characteristics of the liquefaction features (e.g., type, width, lateral continuity, and orientation) were recorded. The stratigraphic context, soil development, and weathering characteristics of liquefaction features were documented, and deformation structures related to liquefaction photographed. At liquefaction sites and other nearby sites, samples collected for ^{14}C and OSL dating were labeled and their stratigraphic positions recorded. Information about the river segments surveyed, including exposure, sediment condition and age, presence or absence of liquefaction features, and estimated ages of features is summarized in Table 3-1 and more detailed information about individual study sites is provided in Table A1 of Appendix A.

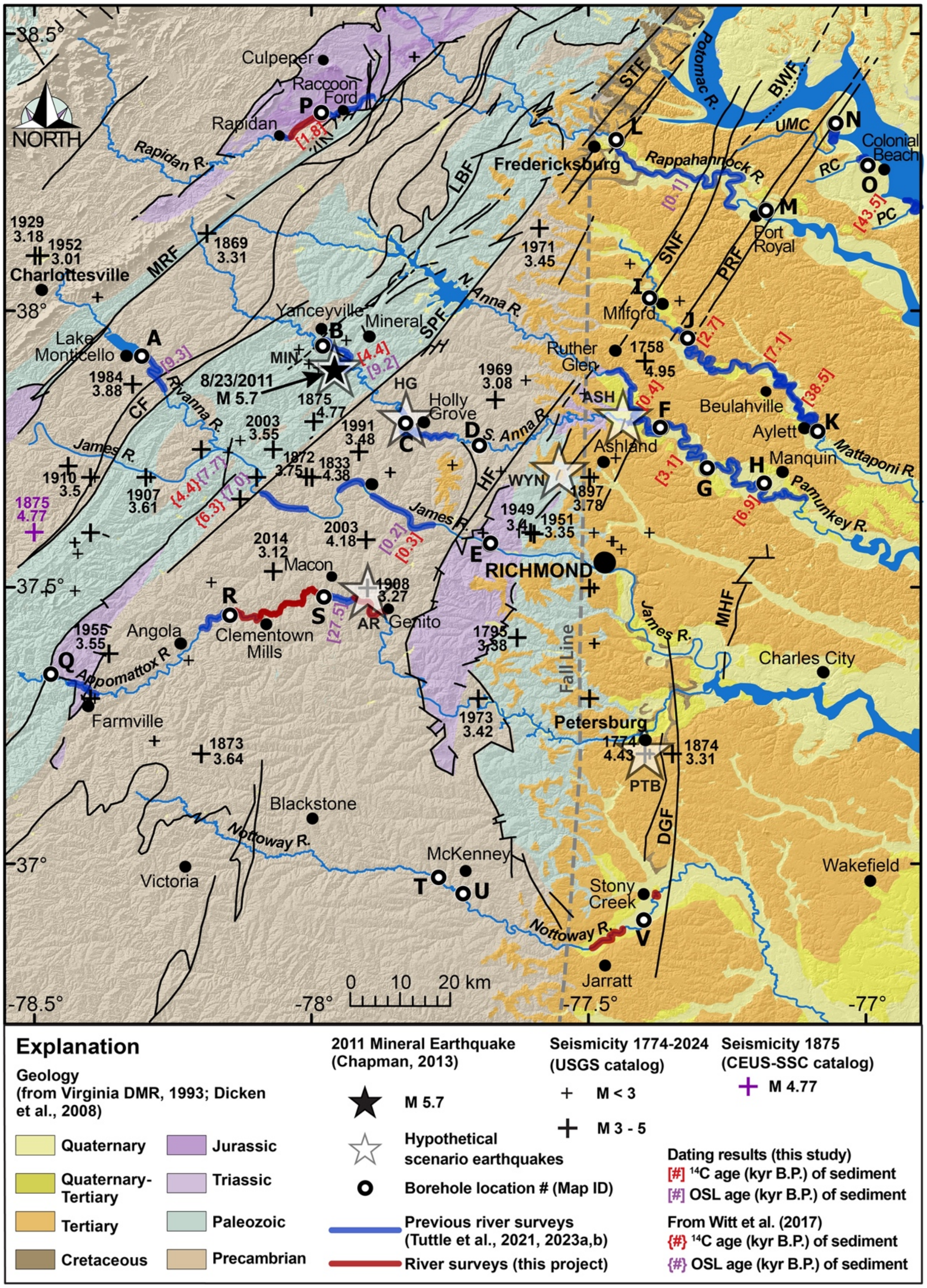

Figure 3-1: Map of CVSZ and surrounding region showing seismicity including 2011 Mineral earthquake, portions of rivers surveyed for liquefaction during this study (red lines) and previous study (purple lines), and locations of boreholes logs and geotechnical data used to evaluate scenario earthquakes using liquefaction potential analysis. For hypothetical scenario earthquakes locations, AR=Appomattox River, ASH=Ashland, MIN=Mineral, PTB=Petersburg, and WYN=Wyndham Forest.

Table 3-1: Summary Information on River Surveys Including Exposure, Sedimentary Conditions, and Liquefaction Features

River Surveys Locations Distance	Cutbank Exposure	Suitable Conditions	Sediment Age[1]	Liquefaction Features	Estimated Age of Features
Southern CVSZ					
Appomattox R. Between Angola & Genito 33 km	Fair to good, especially in river bends, except for lowermost 6 km near Genito; cutbanks range from 4-5 m high	Favorable conditions between Angola and Genito; alluvium – clay, clayey silt, and sandy silt underlain by sand and pebbly sand	Modern to 86,440 yr BP; Holocene & Late Pleisto-cene	Unweathered sand dikes; weathered sand dikes & intruded krotovinas	Historical, 2,640 yr B.P. ± 80 BP, and possibly Middle-Late Pleistocene
Nottoway R. Near Jarrat & Stony Creek 9 km	Poor to very poor; most banks covered by recent flood deposit; few exposures provid-ed by steep cut-banks, tight river bends, slumps; cutbanks range from 3-5 m high	Favorable along Jarratt segment: alluvium – clayey silt & silt underlain by sand. Not favorable along Stony Creek segment: alluvium – mottled silty sand, sand, and cobbley-pebbly sand	140-170 yr BP & >39,940 yr BP; Late Holocene & Late Pleisto-cene	None	Not applicable
Northern CVSZ					
Rapidan Between Town of Rapidan & Racoon Ford 10 km	Fair; few expo-sures in 3-4.5 m terrace in cut-banks in river bends & slump scarps	Yes, Holocene alluvium but only 6 m thick; interbedded silt & sand or silt with interbeds of sand	0-1820 yr BP Modern & Late Holocene	SSDs at two sites and one small sand dike	Historical 1735-1640 C.E

[1] Sediment ages (rounded to nearest decade) of samples collected from river cutbanks; may not reflect the maximum age of sediment exposed or underlying the cutbanks.

3.2 Dating

Narrowly constraining the ages of liquefaction features in the CVSZ is challenging. Most of the liquefaction features in the region are sand dikes and dating is often limited to maximum constraining ages that can be hundreds to thousands of years older than the dikes. In addition, organic material for ^{14}C dating is not always available at liquefaction sites. Therefore, OSL dating of sediment, which is always present, is employed as well as ^{14}C dating of organic samples. Dating results from this and previous studies (Tuttle et al. 20021, 2023a,b) used to correlate features across the region are provided in Appendix B.

Beta-Analytic, Inc. performed ^{14}C dating of organic samples using accelerator mass-spectrometry and calibrated ^{14}C ages using the high probability density range method and the INTCAL20 database (e.g., Bronk Ramsey, 2009; Reimer et al., 2020). Results of ^{14}C dating are provided in Tables B1 and B2 of Appendix B. Geoluminescence Dating Laboratory at Baylor University carried out the OSL dating and calculated systematic and random errors at one standard deviation by the Luminescence Dating and Age Calculator at https://www.baylor.edu/geosciences/index.php?id=962356 (Liang and Forman, 2019). Results of OSL dating are provided in Tables B3 and B4. Due to improvements in methodology during the course of this study (e.g., algorithms that optimize equivalent dose determinations and more robust statistical analyses to reduce errors), some of the OSL ages were recalculated. Unlike ^{14}C ages, OSL ages reflect the mean with error ranges at 1 standard deviation. In order to use both ^{14}C and OSL dating results to estimate the ages of liquefaction features, and thus the timing of paleoearthquakes, ^{14}C ages with error ranges of 1 standard deviation are used in this analysis.

3.3 Analysis and Interpretation of Results

As observed during the previous study (Tuttle et al., 2021), liquefaction features in the CVSZ are limited to mostly small (<10 cm) sand dikes and sills and to soft-sediment deformation structures such as sand diapirs and pseudonodules. Although no sand blows have been found, that is not to say that no sand blows formed during the liquefaction events. Any small sand blow that formed is likely to have been removed by erosion during flooding or destroyed by bioturbation over the course of decades, leaving only subsurface features as evidence of past events. The upper portions and margins of many dikes have been bioturbated, making it difficult to determine how high in the sediment profile the dikes intruded. In addition, the Holocene and Late Pleistocene deposits, including contacts between deposits in which the liquefaction features formed, are also bioturbated. As a result, there are few opportunities to obtain minimum constraining ages from deposits that clearly post-date the formation of liquefaction features. Therefore, age estimates of liquefaction features are based on a few minimum constraining ages and many more maximum constraining ages that are not necessarily close in age.

The number and timing of liquefaction-inducing events are based on age estimates, crosscutting relationships, and weathering characteristics of liquefaction features. Liquefaction features with well-constrained age estimates are given more weight in estimating the timing of past earthquakes. Only small, unweathered dikes have been observed crosscutting larger weathered (mottled and bioturbated) dikes. No crosscutting relationships between weathered liquefaction features have been observed. Therefore, most unweathered features are thought to reflect historical earthquakes and most weathered features are attributed to a paleoearthquake whose timing is based on a few, relatively close, minimum and maximum constraining ages.

For this study, newly found and dated liquefaction features are considered along with previously documented liquefaction features to reassess the timing, locations, and magnitudes of earthquakes that may be responsible for their formation. Liquefaction features are correlated across the region based on their estimated ages and weathering characteristics. The distribution and relative size of similar-age features help to identify likely source areas for past events. Information about liquefaction features, including dike width, average dike width, weathering, age constraints, and event timing is summarized in Table 3-2. Information gathered about liquefaction sites and features was entered into a geodatabase and ArcGIS used to generate a map showing the locations, sizes, and estimated ages of liquefaction features (Figure 1-1).

Table 3-2: Summary of Earthquake-Induced Liquefaction Features, Age Information, and Event Timing (this study and Tuttle et al., 2021, 2023a,b)

River Name	Liquefaction Features[1]	Dike Width (cm)	Average Dike Width (cm)[2]	Weathering	Age Constraint Yr B.P. (1950)[3]	Event Timing
Appomattox	Sand dikes	2	2	Relatively unweathered	NA	Historical
		0.5-12	3.9	Bioturbated & mottled	2,560-3,615 <4,235	2,640 yr B.P. ± 80 yr
					<13,675 to <86,440	Holocene-Late Pleistocene
James	Sand dikes & SSDs	0.6-3	1.8	Some mottling	<270	Historical
Mattaponi	Sand dikes	0.2-14	3.8	Bioturbated & mottled	<2710	2,640 yr B.P. ± 80 yr
					<7155	Holocene
Pamunkey	Sand dikes & SSDs	0.5-4	2.3	Slight iron staining & bioturbation	<310, <2090	Historical
	Sand dikes	2-20	6.3 (4, if largest dike excluded)	Bioturbated & mottled	<3030	2,640 yr B.P. ± 80 yr
					<6880, <8380	Holocene
So. Anna 2011	Sand dike	1	1	Slight iron staining	NA	A.D. 2011
So. Anna Holly Grove	Sand dikes	1-4	2.6	Bioturbated & mottled	<8695	Holocene
So. Anna Mineral	Sand dikes	1-4	2.3	Bioturbated & mottled	<5890	Holocene
Stigger-Rivanna	Sand dikes	1-2.7	1.8	Bioturbated & mottled	<11,435-12,555	Holocene
Rapidan	Sand dike & SSDs	1	1	Gleyed Iron stained	215-310	Historical 1735-1640 C.E.

[1] Only liquefaction features with assigned confidence values of 1 (high) or 2 (medium) included in this table.

[2] Because there can be a range of dike widths for any given liquefaction site, average dike widths calculated for river segments may better reflect trends in liquefaction severity.

[3] Calibrated ^{14}C ages and OSL ages in years B.P. or before A.D. 1950; rounded to the nearest half decade; < = after, > = before. NA – Not applicable.

3.4 Evaluation of Scenario Earthquakes

Scenario earthquakes at hypothetical sources are evaluated to help constrain sources and magnitudes of paleoearthquakes responsible for liquefaction features across the region, including newly found features on the Appomattox and Rapidan rivers. The hypothetical sources include Macon near the weathered sand dikes on the Appomattox River and Wyndham Forest halfway between weathered sand dikes on the Appomattox and Mattaponi rivers, in addition to previously selected hypothetical sources near the 2011 Mineral, VA, earthquake, Holly Grove near the middle of the distribution of liquefaction features, and Ashland where a cluster of small earthquakes have been recorded since 1974 (Figure 3-1).

Liquefaction potential analysis is performed to determine whether or not scenario earthquakes of certain magnitudes and distances are likely or not to induce liquefaction along the various rivers. The cyclic stress method (e.g., Seed and Idriss, 1971 and 1982; Youd and Idriss, 2001; Cetin et al., 2004; Idriss and Boulanger, 2004; Green et al., 2005; Robertson, 2010; Juang et al., 2017; Juang and Jiang, 2000) is used in the analysis, and regionally appropriate ground motion prediction equations (Atkinson and Boore, 2011; Atkinson et al., 2012) are used to calculate peak ground accelerations for scenario earthquakes. Site amplification related to soil conditions is factored into liquefaction potential analysis but does not replace response analysis using site-specific velocity profiles. A detailed description of the cyclic stress method used in this study can be found in the electronic supplement of Tuttle et al. (2021) or Appendix E of U.S. Nuclear Regulatory Commission, RIL-2023-04 (Tuttle et al., 2023a).

Geotechnical data used in the liquefaction analysis was gleaned from borehole logs collected at bridge crossings of river segments that were surveyed for liquefaction features (Figure 3-1; Tables C-1 and C-2 in Appendix C). The borehole logs were provided by the Virginia Department of Transportation. In central Virginia river valleys, the water table typically occurs within a meter of the ground surface, but can drop several meters during periods of drought (Kempthorne and Myers, 2006; https://waterdata.usgs.gov/nwis/gw). Therefore, water table depths of 1 m and 3 m are used in most of the analyses, though only 1 m water table depth is used in the analyses for historical scenario earthquakes. The results of the evaluations of scenario earthquakes at various hypothetical sources are summarized in Table 3-3 and more detailed results are provided in Tables D1-D7 in Appendix D.

Table 3-3: Summary of Magnitude Estimates for Historical and Paleo Earthquakes

Earthquake	Previous Results (Tuttle et al., 2021)		Liquefaction Potential Analysis[1]	
	2 Events	1 Event	3 Events	1 Event
Historical – 1690 ± 50 yr C.E.				**M** 5.5-5.75
Historical – 1758, 1774, 1875 C.E.	**M** 5.0-5.25	**M** 5.75	**M** 5.25-5.5	**M** 5.75-6.0
Paleo – 2,640 ± 80 yr B.P.	**M** 6.0 & **M** 6.25	**M** 6.5-6.75	**M** 6.25-6.5	**M** 6.5-6.75

[1] Preferred magnitude estimates are shaded gray.

4 RIVER SURVEYS FOR AND DATING OF LIQUEFACTION FEATURES

Building on results of prior investigations, this study includes additional survey upstream and downstream from the liquefaction features found on the Appomattox River, survey downstream from the liquefaction features found on the Nottoway River, and resurvey of a portion of the Rapidan River to look for additional liquefaction features (Figures 1-1 and 3-1). Also, sites of possible liquefaction features along the Rapidan River and a liquefaction site along Stigger Creek, a tributary to the Rivanna River, were revisited and samples collected for OSL dating to better constrain the ages of the features found during the previous studies. River surveys and dating of liquefaction features are discussed below.

4.1 Appomattox River

Additional survey for liquefaction features was conducted along several segments of the Appomattox River, including 7 km between Angola and Clementine Mills, 19 km between Clementine Mills and Macon, and 7 km between Macon and Genito for a total of 33 km (Figure 3-1). Along these segments of the river, Holocene alluvium is inset into Quaternary and Tertiary deposits (Mixon et al., 1989).

River cutbanks ranged from 4-5 m in height with the upper 0.5-2 m covered with vegetation (Table 3-1; Table A-1 in Appendix A). Otherwise exposure was fair to good, especially in river bends, except for the lower 6 km of the Macon-Genito segment where more of the banks were vegetated. Most of the cutbanks revealed an upper unit of drab silt, or sand fining upward to silt, underlain by a lower unit of mottled, silty sand, silt, and clayey silt. Layers of sand and pebbly sand sometimes occurred near the bottom of the cutbank. Probing up to 1.6 m below the cutbanks, silt, sandy silt, and sand were encountered, with sand often becoming more common and coarser with depth. At sites where the river channel approached the margin of the floodplain, bedrock was often encountered 1-1.5 m below the cutbank during probing. Occasionally, rock cropped out along the river banks.

Liquefaction features were found along all three segments searched where the sediment conditions are favorable for the formation of liquefaction features (Figures 1-1 and 3-1). Along the Angola-Clementine Mills segment, the sediment section is about 4-5 m thick and sand and pebbly sand, 0.25-1.2 m thick, occur below clay, clayey silt, and sandy silt in several locations. Along the Clementine Mills-Macon segment and the upper several km of the Macon-Genito segment, conditions are similar and even more favorable where sand and pebbly sand becomes thicker and more common.

As found previously, there appears to be two generations of liquefaction features, primarily sand dikes, along the Appomattox River. The few younger sand dikes are relatively unweathered, crosscut older features, and range up to 2 cm in width (Table 3-2). These features are interpreted as historical in age due to the lack of weathering. The older sand dikes are very weathered (mottled and bioturbated) and range from 0.5-12 cm in width. At site AR8, sand dikes crosscut silt with manganese nodules and approach a depositional contact between a silt loam and silty, very fine sand above. Dating of samples AR8-OSL1 (BG5409) and AR8-OSL2 (BG5408) collected above and below the contact, respectively, provide minimum and maximum constraining ages of 2,655 ± 95 and 3,490 ± 125 yr B.P. (Figure 4-1; Table 3-2; Table B-4, age recalculated, in Appendix B), suggesting that the older, weathered sand dikes at the site formed between 2,560 and 3,615 yr B.P. Dating of older, weathered features at other sites along the river is limited to maximum

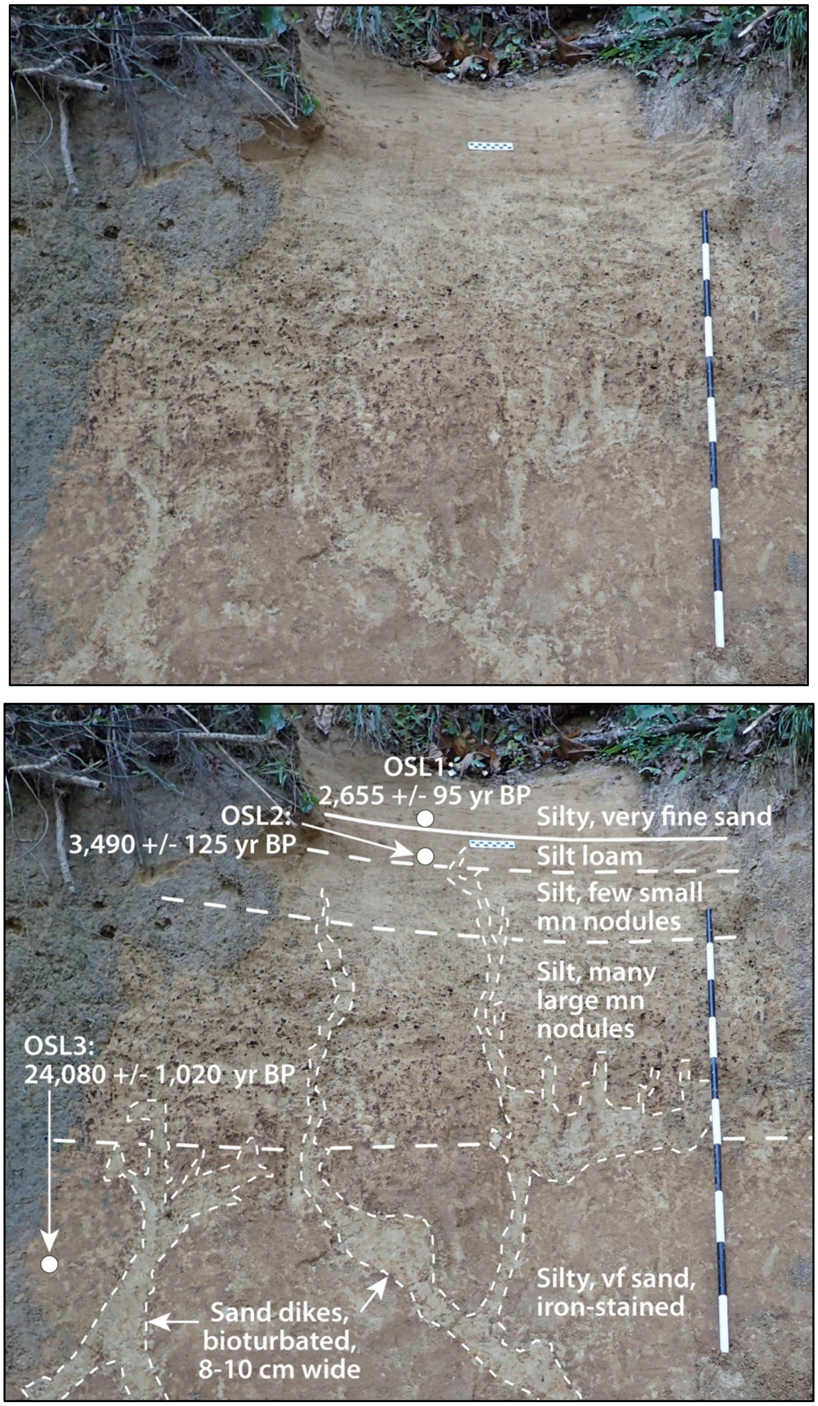

Figure 4-1: Photographs (upper unannotated; lower annotated) of weathered sand dikes exposed in the cutbank at site AR8 along the Appomattox River (from Tuttle et al., 2023a). The mottled and bioturbated sand dikes narrow and branch upward. None of the dikes crosscut the depositional boundary between silt loam and overlying, less weathered, silty sand. OSL dating of AR8-OSL1 and AR8-OSL2 on either side of that depositional boundary provide minimum and maximum constraining ages (recalculated for this study) of 2,560 yr B.P. and 3,615 yr B.P., respectively, for the dikes. Black and white intervals of the meter stick represent decimeters and squares of the small scale represent centimeters.

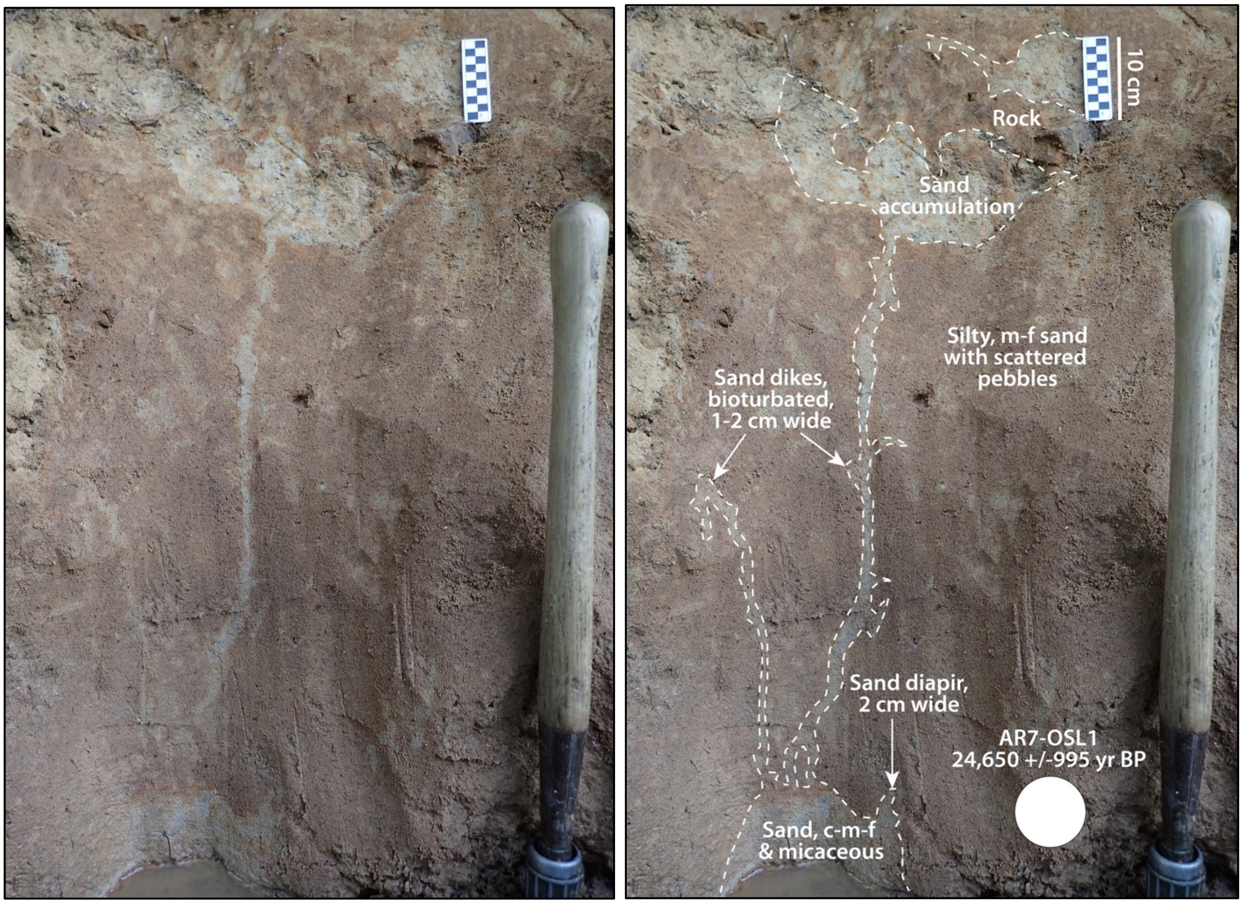

Figure 4-2: Photographs (left unannotated; right annotated) of sand dikes and diapir exposed in lower 70 cm of cutbank at site AR7 along the Macon-Genito segment of the Appomattox River. Dating of AR7-OSL1 provides a maximum constraining age (recalculated for this study) of 24,650 +/- 995 yr B.P. One of the dikes extended to 50 cm above the river level where sand accumulated below a rock fragment, wrapped around the fragment, and pinched out 65 cm above the river level. This phenomenon of sand accumulation below obstacles was observed in excavations of liquefaction features in Ferland, Quebec, where the 1988 M 5.9 Saguenay earthquake induced liquefaction (Tuttle et al., 1990). Black and white squares of small scale represent centimeters and shovel handle is 50 cm long.

constraining ages that range from ca. 4.2 to 86.4 ka (Figures 4-2 and 4-3; Table 3-2; Table A-1 in Appendix A).

There are no apparent crosscutting relations among the older liquefaction features, and they exhibit similar pedogenic effects; thus, they are hypothesized to be contemporaneous. However, it remains a viable hypothesis that some of these features may have formed during different events, spanning the Middle Holocene and Late Pleistocene.

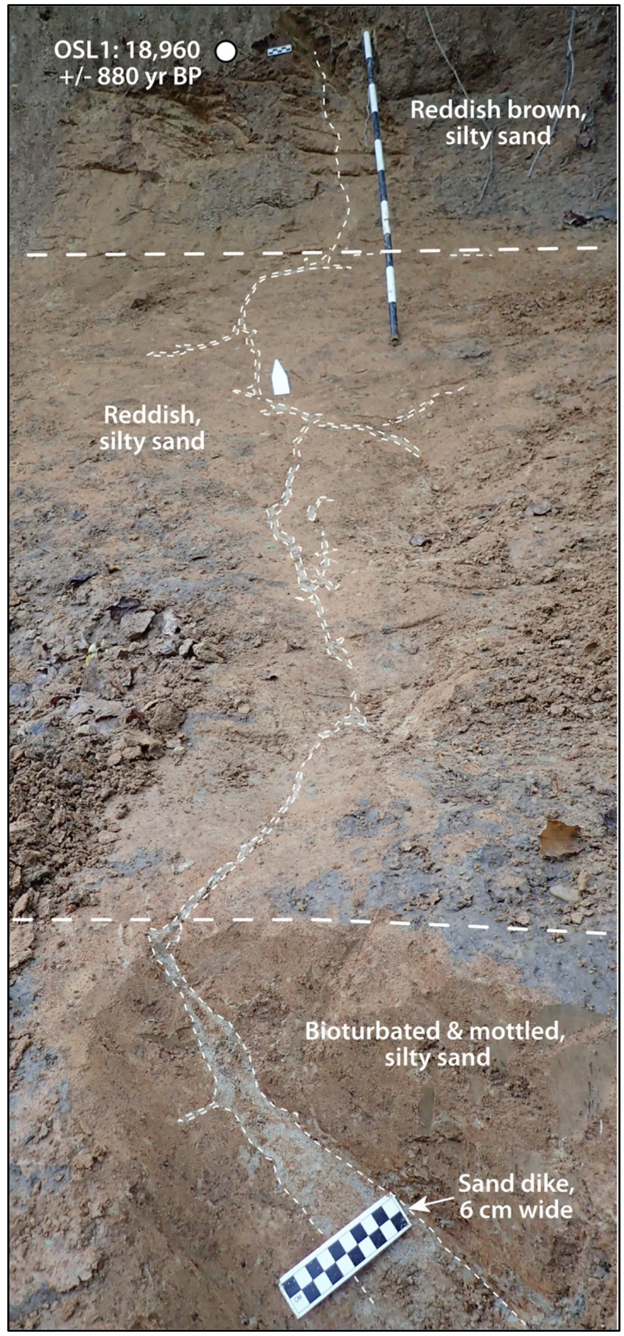

Figure 4-3: Photographs (left unannotated; right annotated) of one of several sand dikes exposed in the cutbank at site AR108b along the Clementown Mills-Macon segment of the Appomattox River. This dike narrows upward as it crosscuts bioturbated, mottled, and iron-stained silty sand. The dike becomes difficult to trace in the more weathered upper portion of the cutbank where it ends, or has been destroyed by bioturbation, at 1.55 m below the top of the cutbank. At nearby site AR108a in the same cutbank, sand dikes originate in a layer of sand at water level. Dating of AR108b-OSL1 indicates that the dikes exposed in this cutbank formed since 18,960 +/- 880 yr B.P. yr B.P. Black and white squares on the small scales represent centimeters and black and white intervals on the meter stick represent decimenters.

4.2 <u>Nottoway River</u>

The survey along the Nottoway River was conducted east of the Fall Line and downstream from the sand dikes previously found near McKenney (Carter et al. 2022). The survey included 7.7 km downstream from Jarratt and 1.3 km east of Stony Creek for a total of 9 km (Figure 1-1; Table 3-1). Along these portions of the river, Holocene and Pleistocene alluvium is inset into older Pleistocene terraces and plains (Mixon et al., 1989). River cutbanks ranged from 3-5 m in height.

Unfortunately, Tropical Storm Ophelia passed over Virginia several weeks prior to field work. The combination of heavy rainfall and storm surge along the coast caused prolonged flooding of the Nottoway River, especially east of the Fall Line where our survey was conducted. As a result, most of the river cutbanks were covered with a recent deposit of mud. The few exposures of Holocene and Pleistocene alluvium occurred on steeper cutbanks or in tight river bends and recent slump scarps along the base of the cutbanks.

Along the Jarratt section of the river, brown sandy loam was underlain by mottled clayey silt, silt, or sand. In a few instances, clayey silt was underlain by sand (Table 3-1). Probing encountered sand or silty sand towards the base of the sediment section, ferricrete in some of the sandy layers, and bedrock within 1.1 m below the cutbank. At site NR1 along this section, dating of samples NR1-OSL1 (BG5826) and NR1-OSL2 (BG5827) indicate that clayey silt of the upper part of the cutbank was deposited 155 ± 15 yr B.P. and that coarse-medium sand of the lower part of the cutbank was deposited >39,940 yr B.P. (Figure 4-4; Table A-1 and Table B-3). Along the Stony Creek section, several exposures in river bends revealed reddish sand overlying cobbly-pebbly sand. Probing indicated that coarse sediment continued with depth and ferricrete had formed within 1.2 m below the base of the cutbank.

No liquefaction features were found along either section of the river; however, this is not surprising given the poor exposure resulting from recent deposition of flood deposit on the cutbanks. The sediment conditions along the Jarratt section appear conducive to the formation of liquefaction features and therefore warrant a second look when the cutbanks are better exposed after the flood deposit has been removed by erosion. The sediment conditions along the Stony Creek section, do not appear to be favorable for the formation of liquefaction features, and therefore, may not warrant additional reconnaissance.

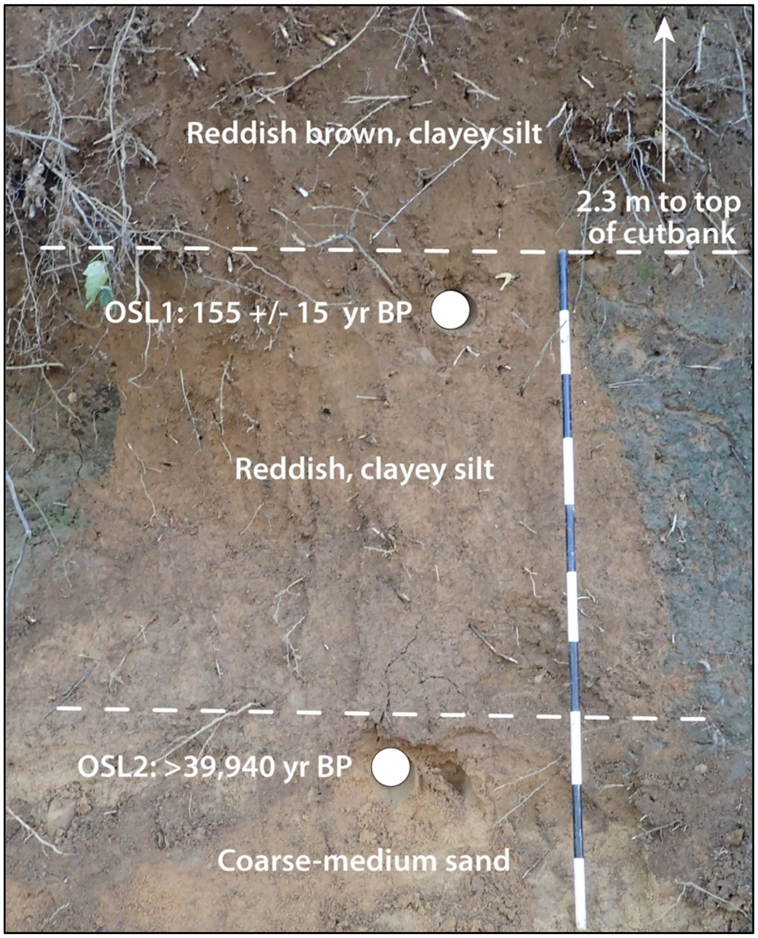

Figure 4-4: Photograph at site NR1 of cutbank exposure in 4-m-high river terrace along Nottoway River. A few exposures such as this one along the Jarratt segment of the river, where clayey silt overlies sand, suggest that conditions are favorable for the formation of liquefaction features. Unfortunately, most of the banks of the Nottoway were covered by a recent flood deposit. For scale, black and white intervals of meter stick are 10 cm long.

4.3 Rapidan River

In 2021, survey for liquefaction features along was conducted along 23 km of the Rapidan River downstream from the town of Rapidan (Figure 1-1; Tuttle et al., 2003a). Along this portion of the river, Holocene and Pleistocene alluvium has been described as being about 6 m thick and composed of gravel and sand filling channels at the base of fining-upward sequences (Table 3-1; Mixon et al., 2000). Also, Pleistocene-Pliocene terrace deposits, up to 10 m thick, include gravel, sand, silt, and clay underlying lowland benches 6-20 m above the adjacent flood plains. During the survey, two terrace levels were noted along the river (Table 3-1). There were relatively few cutbank exposures, most of which occurred in river bends and in the lower terrace, which was 3.0-4.5 m above the river level. The upper portions of the banks were mostly vegetated and exposures occurred in the lower half or third of the banks. The few exposures revealed interbedded silt and iron-stained sand or mottled silt with a few thin layers of sand. Occasionally, sandy silt or pebbly sand with a few cobbles occurred near the base of the cutbanks. Probing below the cutbanks, silt or interbedded silt and sand continued for only 0.5-1.5 m where bedrock was usually encountered.

In 2023, a 10-km portion of the river was resurveyed to search for additional liquefaction features and to collect samples for dating. Unfortunately, exposure was even worse than in 2021 due to vegetative growth even on the lower portion of many of the cutbanks. No new liquefaction sites were found but sites RnR1 and RnR3, where SSDs likely related to earthquake-induced liquefaction had been found in 2021, were relocated (Figure 1-1; Table 3-2; Table A-1 in Appendix A).

At site RnR1, pseudonodules or rounded masses of sand extended downward into the underlying silty sand layer and diapirs of the silty sand extended upward into the overlying sand layer (Figure 4-5). In addition, there were a few flames rising from the sand layer into overlying silt layers. Previously, ^{14}C dating of organic samples RnR1-C2 (BA609016) and RnR1-C1 (BA609015) collected 30 cm above and 35 cm below the SSDs, respectively, yielded minimum and maximum constraining ages of 142 yr B.P. and 1818 yr B.P. (Table B-1 in Appendix B). In 2023, sediment samples RnR1-OSL1 (BG5823) and RnR1-OSL2 (BG5824) were collected 20 cm above and 10 cm below the SSD (Figure 4-5). OSL dating of the samples returned ages of 230 ± 15 yr B.P. and 295 ± 15 yr B.P., suggesting that the SSDs formed between 215 and 310 yr B.P. (Table B-3).

At site RnR3, a small sand dike, 1 cm wide at the base of the cutbank, intruded 25 cm into the overlying mottled silt and branched upward before becoming difficult to trace due to bioturbation. In addition, a small flame structure, which verged upstream, extended upward from a thin layer of sand into the overlying silt. These features suggest that liquefaction may have occurred at the site. Probing below the cutbank, interbedded silt and sand continued for only 0.5 m where bedrock was encountered. In 2023, sediment samples were collected at this site for OSL dating. Dating of sample RnR3-OSL1 (BG5825) from a sandy layer crosscut by the dike yielded an age of 330 ± 15 yr B.P., suggesting that the features formed since 345 yr B.P. (Table B-3).

The combination of a sand dike and SSDs at the two sites suggest an earthquake origin. Given age constraints, the features could have formed during the same event between 1735-1640 C.E. (Table 3-2). Similar SSDs have been attributed to liquefaction (Sims, 1975, 2012; Tuttle et al., 2019) resulting from earthquakes of Modified Mercalli intensities of VIII (Sims, 1973) or **M** $\geq$5 (Uner, 2014). Although conditions conducive to the formation of liquefaction features do exist along the river, they are limited by the distribution and thickness of sand. Also, the sediment section appears to be fairly young and may limit the record of earthquakes to the past 2 kyr.

(a)

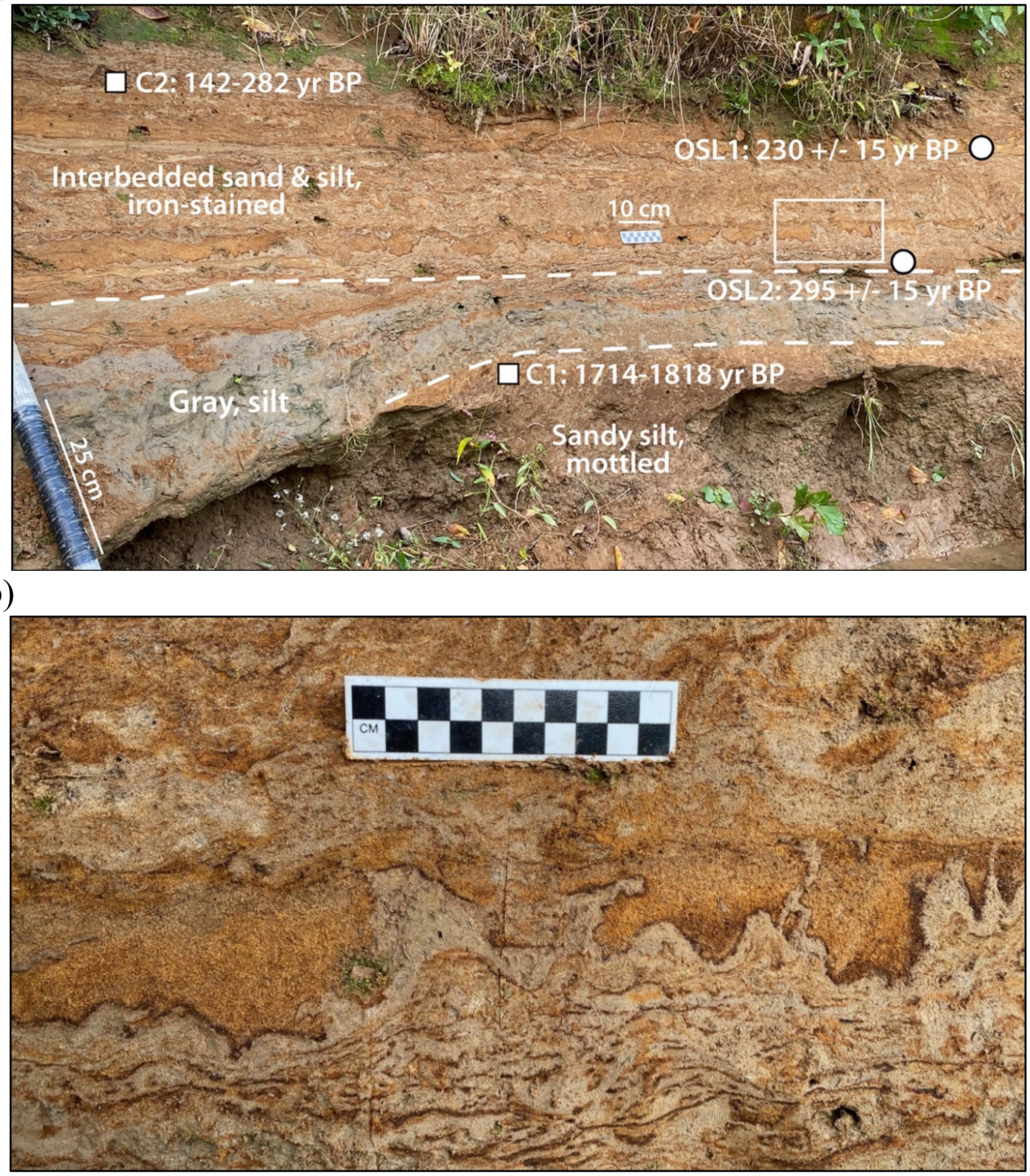

(b)

Figure 4-5: Photographs of SSDs at site RnR1 along the Rapidan River west of Fredericksburg: (a) Photograph of the lower 1.5 m of the cutbank bank shows SSDs in iron-stained interbedded sand and silt. OSL dating of sediment samples RnR1-OSL1 and RnR1-OSL2 collected above and below the SSDs, respectively, indicates that they formed between 215-310 yr B.P. (b) Closeup photograph of SSDs showing pseudonodules of sand sinking downward into underlying silty sand and diapirs of silty sand extending upward into the overlying sand layer. Both layers may have liquefied and mobilized, leading to the formation of the SSDs. Area of closeup of SSDs indicated by white rectangle in (a).

4.4 Rivanna River-Stigger Creek

West of Mineral, a site of liquefaction along Stigger Creek near its confluence with the Rivanna River, was originally found in the 1990s (Figure 1-1; Obermeier and McNulty, 1998; Dominion, 2004). Liquefaction features at the site were verified following the 2011 Mineral earthquake and dating of sample RR-SC1-OSL1 (BG4002.B) collected from the source strata for several sand dikes returned an OSL age of 11,010 ± 425 yr B.P. (Table B-4, age recalculated) (Tuttle et al., 2021). During this study, the site, RR-SC1, was revisited to collect additional samples for OSL dating but it was overgrown with vegetation. About 25 m upstream, however, an actively eroding cutbank revealed a similar sedimentary section crosscut by several bioturbated and mottled sand dikes. At this site, RR-SC2, three sediment samples were collected from the section, including from the source strata for the dikes, a mottled silty fine sand crosscut by the dikes, and an overlying reddish silt in which the most extensive dike terminated highest in the section (Figure 4-6; Table A-1 of Appendix A). The OSL ages for the three samples are consistent with one another, showing that the sediments young upward. The uppermost sample RR-SC2-OSL1 (BG5802) yielded an age of 12,030 ± 525 yr B.P., suggesting that the sand dikes at this site and nearby site RR-SC1 formed since ca. 12.6 ka. (Table 3-2; Table A-1; Table B-3).

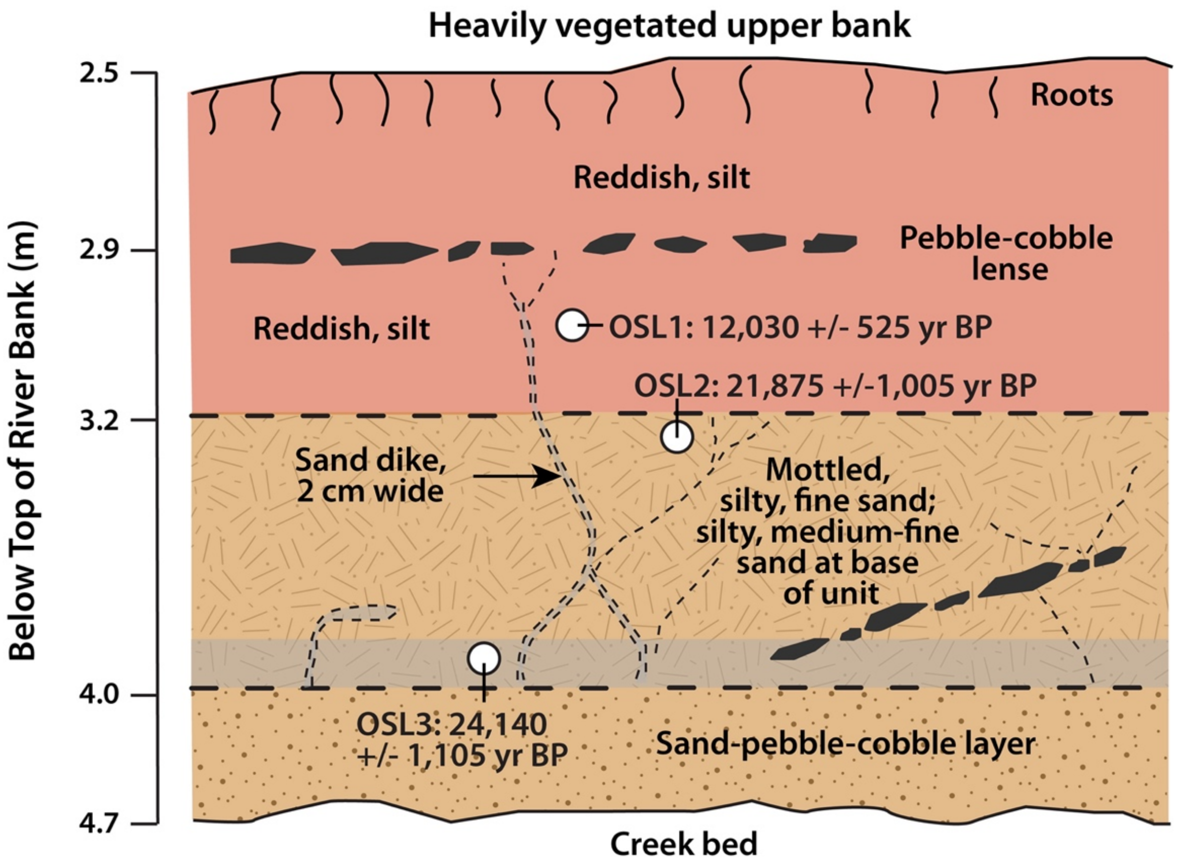

Figure 4-6: Sketch of cutbank exposure at site RR-SC2 along Stigger Creek near its confluence with the Rivanna River west of Mineral. OSL dating at the site indicates that the sand dikes formed since 12,030 +/- 525 yr B.P. This site is located ~25 m upstream from RR-SC1 which was heavily vegetated during field work in 2023. Previous OSL dating at RR-SC1 suggested that sand dikes at that site formed since 11,010 +/- 425 yr B.P.

5 UPDATE ON THE EARTHQUAKE POTENTIAL OF THE CVSZ

Findings during this study add confidence to the previous interpretation that there was at least one large paleoearthquake in the CVSZ during the Late Holocene, narrows the age estimate of the paleoearthquake, and further constrains estimates of its source area and magnitude. Also, findings suggest an additional earthquake source west of Fredericksburg that may have produced a moderate earthquake during the early colonial period.

5.1 Earthquake-Induced Liquefaction and Event Timing

During this study, likely liquefaction features were studied along the Appomattox River west of Richmond and along the Rapidan River west of Fredericksburg (Figure 1-1; Table 2-3). Along the Appomattox River, at least two generations of liquefaction features, including sand dikes and intruded krotovina, occur in Holocene and Late Pleistocene deposits. The older features are bioturbated and mottled; whereas, the younger features are relatively unweathered and crosscut the older features. Given their similarity to historical sand dikes on the James and Pamunkey rivers, the unweathered sand dikes are thought to have formed during one of the historical earthquakes in the CVSZ, most likely the 1758, 1774, or 1875 C.E. event.

On the basis of OSL dating of host sediment, a few of the weathered features along the Appomattox River are estimated to have formed between 2,560 and 3,615 yr B.P. This age estimate overlaps with maximum constraining ages of 2,710 yr B.P. and 3,030 yr B.P. for some of the weathered liquefaction features along the Mattaponi and Pamunkey rivers (Table 3-2; Table A-1 in Appendix A). By combining the most restrictive minimum (2,560 yr B.P.) and maximum (2710 yr B.P.) constraining ages for the weathered features along the Appomattox, Mattaponi and Pamunkey rivers, the timing of the paleoearthquake is estimated to be ca. 2,640 ± 80 yr B.P.

There are other weathered features along all three rivers, and along the South Anna River and Rivanna River-Stigger Creek, with older maximum constraining ages, spanning from 4,235-86,440 yr B.P. Given the lack of crosscutting relationships or differences in weathering characteristics, however, the weathered features along all five rivers may have formed as a result of the same contemporaneous paleoearthquake. This interpretation is supported by the size distribution of the weathered sand dikes. Average dike width is greatest, 6.3 cm (or 4 cm if the largest dike width of 20 cm is excluded as an outlier) for the Pamunkey River and somewhat smaller, 3.8 and 3.9 cm, for the Mattaponi and Appomattox rivers, north and south of the Pamunkey River (Table 3-2). In addition, average dike width decreases towards the west from 6.3 cm for the Pamunkey River, 2.6 cm for the South Anna near Holly Grove, 2.3 cm for the South Anna near Mineral, to 1.8 cm for Rivanna River-Stigger Creek. This size distribution, with average dike width decreasing away from a somewhat central point is consistent with a liquefaction field resulting from one event with the larger features more likely occurring near the source of the earthquake.

Poor age constraints of many of the weathered features would allow for earlier earthquakes, but currently, there is no unequivocal evidence such as crosscutting relationships to support multiple events large enough to induce liquefaction during the Middle-Late Holocene and Late Pleistocene (Table 3-2).

Along the Rapidan River, liquefaction features, including one small sand dike, pseudonodules, diapirs, and flames, occur in modern and Late Holocene deposits and are estimated to have formed ca. 1690 ± 50 yr C.E. There is no known historical earthquake in the CVSZ or surrounding region during this time period. However, a map by L'Isle published in 1718 C.E. labels the area in the vicinity of the Rapidan River as "terre tremblante" or "trembling earth" (Figure 5-1), suggesting that early colonists had experienced earthquakes in the area.

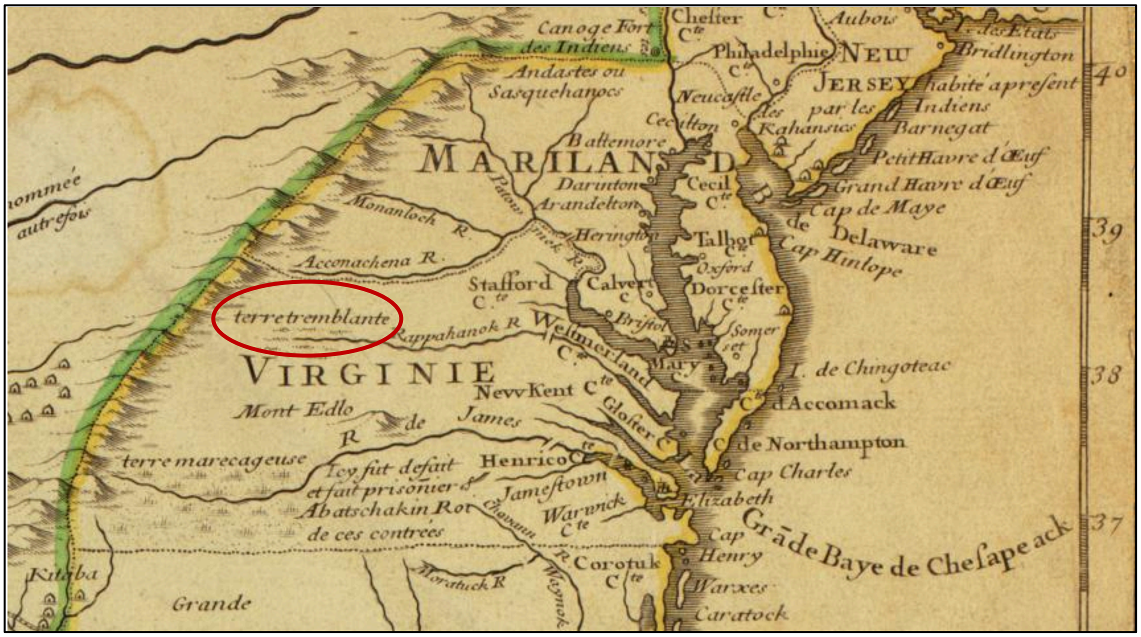

Figure 5-1: Map by L'Isle (1718) depicts an area along the western stretch of the Rappahannock River as "terre tremblante" or "trembling earth." This area is in the vicinity of the Rapidan River, a tributary to the Rappahannock River, where likely liquefaction features formed between 215-310 yr B.P. or 1735-1640 C.E.

5.2 Evaluation of Locations and Magnitudes of Past Earthquakes

Building on previous research, scenario earthquakes are evaluated to help further constrain the locations and magnitudes of earthquakes responsible for the formation of the liquefaction features found along the Appomattox and Rapidan rivers.

Relatively unweathered sand dikes along the Appomattox River are thought to have formed during the historical period; whereas, weathered sand dikes formed ca. 2,640 ± 80 yr B.P. Liquefaction potential analysis suggests that the historical liquefaction features along the Appomattox, James, and Pamunkey rivers could have formed during the following: (1) three **M** 5.25-5.5 earthquakes located within 10 km of each group of features, or (2) one **M** 5.75-6.0 earthquake located between the features on the James and Pamunkey rivers (Tables 3-3; Tables D-1 and D-2 in Appendix D). Given that none of the historical earthquakes were estimated to be greater than **M** 5.32 (Table 5-1), it seems very unlikely that one **M** ≥ 5.75 earthquake was responsible for the young liquefaction features on all three rivers. Given the uncertainty in their locations (34-50 km) as well as their magnitudes (Table 5-1; Figure 5-2), it is plausible that some combination of the 1758, 1774, and 1875 C.E. earthquakes were responsible for the features and that these events may have been slightly larger, **M** 5.25-5.5, than previously estimated.

There is now more robust data and observations to better constrain the location and magnitude of the 2,640 ± 80 yr B.P. earthquake reflected by paleoliquefaction features along the Appomattox, Mattaponi, Pamunkey, Rivanna (Stigger Creek), and South Anna rivers. Using liquefaction potential analysis, scenario earthquakes were evaluated for hypothetical source areas near the following: (1) the 2011 Mineral, VA, earthquake, (2) Holly Grove near the middle of the distribution of liquefaction features, (3) Ashland, where a cluster of small earthquakes have been recorded since 1974 and previously noted during studies of the CVSZ, (4) Wyndham Forest, halfway between liquefaction features on the Appomattox and Mattaponi River, and (5) Macon, near some of the larger features on the Appomattox River (Figures 1-1 and 3-1).

Table 5-1: Significant Pre-Instrumental Earthquakes in the CVSZ

Catalog[1]	Yr	Mo	Day	Latitude	Longitude	ERH[2]	Mw[3]	E[M][4]	sigM[5]	M Range
SSC	1758	3	23	37.91°	-77.4°	50		4.95	0.371	4.58 -5.32
USGS	1758	3	23	37.91°	-77.4°		4.95		0.371	4.58 -5.32
SSC	1774	2	21	37.2°	-77.4°	45		4.38	0.152	4.23-4.53
USGS	1774	2	21	37.2°	-77.4°		4.43		0.5	3.93-4.93
SSC	1791	1	15	37.5°	-77.5°	40		2.65	0.515	2.14-3.17
USGS	1791	1	15	37.5°	-77.5°		2.68		0.5	2.18-3.18
SSC	1833	8	27	37.7°	-78.0°	38		4.37	0.146	4.22-4.52
USGS	1833	8	27	37.7°	-78.0°		4.38		0.333	4.05-4.71
SSC	1875	12	23	37.6°	-78.5°	34		4.77	0.316	4.45-5.09
USGS	1875	12	23	37.8°	-78.0°		4.77		0.35	4.42 -5.12

[1] SSC - declustered catalog used in CEUS Seismic Source Characterization Project (EPRI et al., 2012); USGS – declustered catalog used in National Seismic Hazard Maps (Mueller, 2019).

[2] Estimated horizontal location uncertainty (km).

[3] Moment magnitude.

[4] Expected value of moment magnitude.

[5] Standard error in the estimated moment magnitude, E[**M**].

According to the analysis, the paleoliquefaction features along the five rivers could have formed during one earthquake of **M** 6.5-6.75 near either Holly Grove, Macon, or Wyndham Forest or a larger event of **M** 6.75-7.0 near either Mineral or Ashland (Table 3-3; Tables D-3 to D-7 in Appendix D). Alternatively, the features could have formed during three **M** 6.25-6.5 earthquakes centered near Mineral, Holly Grove, and Ashland. If it is assumed that only the weathered dikes on the Appomattox, Mattaponi, and Pamunkey rivers with maximum constraining ages <4240 yr B.P. formed during the ca. 2,640 ± 80 yr B.P event, and all other weathered features are excluded, the analysis suggests that they could be explained by a **M** 6.25 earthquake near Wyndham Forest. In this case, weathered dikes along all five rivers with older maximum constraining ages, would have formed during earlier earthquakes. However, currently there is no unequivocal evidence to support multiple large earthquakes prior to ca 4.2 ka. Therefore, one earthquake of **M** 6.5-6.75 near Holly Grove, Macon, or Wyndham Forest is the preferred interpretation (Table 3-3). This interpretation is supported by the size distribution of the liquefaction features across the region as described in section 5.1.

The size distribution, with the largest average dike width for the Pamunkey River, suggests that the source of the 2,640 ± 80 yr B.P event may be in the Ashland area. However, amplification of ground motion in the Coastal Plain (e.g., Hough, 2012: Pratt et al., 2017), where unconsolidated sediment overlies crystalline bedrock, may have contributed to liquefaction along the Pamunkey

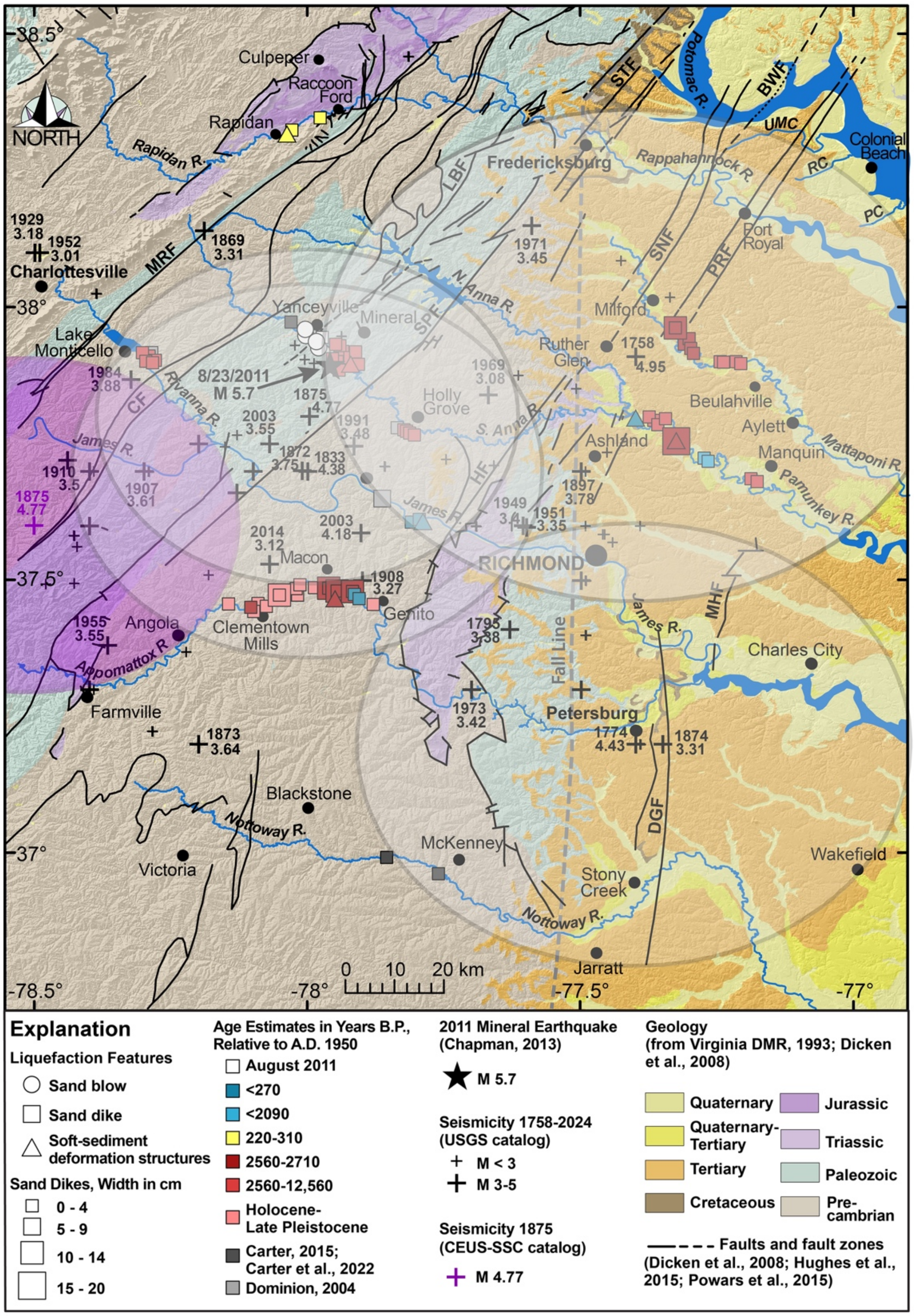

Figure 5-2: Map of the CVSZ showing horizontal or epicentral error ellipses for the 1758, 1774, 1833, and 1875 C.E. pre-instrumental earthquakes according to the CEUS SSC Project earthquake catalog (EPRI et al., 2012; Table 5-1). The horizontal error ellipse of the 1875 earthquake is shown for locations according to both the USGS (Mueller, 2019; Rukstales and Petersen, 2019) and CEUS SSC Project earthquake catalogs. Fault zones: CF=Chopawamsic; LBF=Long Branch; MRF=Mountain Run; SPF=Spotsylvania; HF=Hylas; SNF=Skinkers Neck; PRF= Port Royal; DGF=Dutch Gap; and MHF=Malvern Hill.

and Mattaponi rivers. Average dike width for the Appomattox River is similar to that for the Mattaponi River, but this portion of the Appomattox River is located west of the Fall Line where amplification of ground motion would be less of a factor. Therefore, the source of the event is more likely located closer to Wyndham Forest than to Ashland.

Along the Rapidan River, possible liquefaction features may have formed during a previously unrecognized earthquake ca. 1690 ± 50 yr C.E. This finding along with a map by L'Isle published in 1718 suggests that there is an earthquake source in the area. Liquefaction potential analysis suggests that an earthquake of **M** 5.5-5.75 located within 10 km could have induced liquefaction along the Rapidan River (Table 3-3; Tables D-1 to D-2). Such an event would have been similar in magnitude to the 2011 Mineral earthquake and like the Mineral earthquake only produced relatively small liquefaction features in the epicentral area.

6 CONCLUSIONS

This study contributes to understanding of the earthquake potential of the CVSZ, though uncertainties remain regarding the age of many of the liquefaction features and, to a lesser degree, the regional extent of liquefaction. Dating of weathered liquefaction features along the Appomattox River as well as of weathered features along the Mattaponi and Pamunkey rivers narrows the age estimate to ca. 2,640 ± 80 yr B.P. for a large paleoearthquake thought to have induced liquefaction across the region. The paleoearthquake is interpreted to have been of **M** 6.5-6.75 and located near Wyndham Forest, northwest of Richmond, based on the evaluation of scenario earthquakes and supported by the average width of sand dikes documented along five rivers. Alternatively, three **M** 6.25-6.5 earthquakes centered near Mineral, Holly Grove, and Ashland could account for the formation of the liquefaction features if their size distribution were disregarded. Relatively unweathered liquefaction features found on the Appomattox, James, and Pamunkey rivers are interpreted to have formed as the result of some combination of the historical earthquakes of 1758, 1774, and 1875 C.E. which may have been of **M** 5.25-5.5, slightly larger than previously thought. Dating of liquefaction features found along the Rapidan River provides an age estimate of ca. 1690 ± 50 yr C.E. for a previously unrecognized earthquake in an area depicted on a map published in 1718 C.E. as "terre tremblante" west of Fredericksburg. Liquefaction potential analysis suggests that minor liquefaction along the Rapidan River could have been caused by a local **M** 5.5-5.75 earthquake similar to the 2011 Mineral earthquake.

7 REFERENCES

Atkinson, G., and Boore, D., 2011, Modification to existing ground-motion prediction equations in light of new data, Bulletin of the Seismological Society of America, v. 101, n. 3, p. 1121- 1135.

Atkinson, G., (with input from) J. Adams, G. Rogers, T. Onur, and K. Assatourians, 2012, White paper on development of ground motion prediction equations for Canadian national seismic hazard maps, www.seismotoolbox.ca (Miscellaneous Resources*)*.

Berti, C., Pazzaglia, F.J., Meltzer, A.S., and Harrison, R.W., 2015. Evidence for persistent, cumulative deformation of the Virginia Piedmont in the vicinity of the 23 August, 2011 Mineral earthquake, *in* Horton, J.W., Chapman, M.C., and Green, R.A., eds., The August 23, 2011 Earthquake in Central Virginia and its Significance for Seismic Hazards in Eastern North America. Geological Society of America Special Paper 509, p. 1-14.

Bronk Ramsey, C., 2009, Bayesian analysis of radiocarbon dates, Radiocarbon, v. 51, n. 1, p. 337-360.

Carter, M.W., 2015, Characterizing pedogenic and potential paleoseismic features in South Anna River alluvium: epicentral region of the 2011 earthquake Central Virginia seismic zone, Presentation at the 2015 Virginia Geological Research Symposium.

Carter, M.W., Powell, L., Johnson, J.W., Spears, D.B., Nolan, J.T., Lynn, A.S., 2020, Geotravers along the Nottoway River in southeastern Virginia: New Cooperative geologic mapping on the west half of the Emporia 30X60-minute quadrangle, Joint Northeastern/Southeastern Section Meeting of the Geological Society of America.

Carter, M.W., Tuttle, M.P., Mahan, S., and Merschat, A., 2022, Review of recent and ongoing paleoliquefaction studies in the southeastern US: Results from VA and NC, [abs.] Special Virtual Mini-Conference, AEG, https://www.aegmeetings.org/symposium-schedule.

Cetin, K.O., Seed, R.B., Der Kiureghian, A., Tokimatsu, K., Harder, L.F. Jr, Kayen, R.E., Moss, R.E.S., 2004, SPT-based probabilistic and deterministic assessment of seismic soil liquefaction potential, ASCE Journal of Geotechnical and Environmental Engineering, v. 130, n. 12, p. 1314-1340.

Chapman, M.C., 2013, On the rupture process of the 23 August 2011Virginia earthquake, Bulletin of the Seismological Society of America, v. 103, p. 613-628.

Chapman, M.C., 2015, Magnitude, recurrence interval, and near-source ground motion modeling of the Mineral, Virginia, earthquake of 23 August 2011, *in* Horton, J. W., Jr., Chapman, M. C., and Green, R. A., eds., The 2011 Mineral, Virginia, earthquake, and its significance for seismic hazards in eastern North America, Geological Society of America Special Paper 509, p. 27-45.

Cohen, K.M., S.C. Finney, P.L. Gibbard, and J.-X. Fan, updated 2022, The ICS International Chronostratigraphic Chart, Episodes 36, p. 199-204, http://www.stratigraphy.org/ICSchart/ChronostratChart2022-10.pdf.

Dicken, C.L., Nicholson, S.W., Horton, J.D., Kinney, S.A., Gunther, G., Foose, M.P., Mueller, and J.A.L., 2008, Preliminary integrated geologic map databases for the United States: Delaware, Maryland, New York, Pennsylvania, and Virginia, U.S. Geological Survey, Open-File Report 2005-1325*,* https://pubs.usgs.gov/of/2005/1325/.

Dominion, 2004, Response to request for additional information no. 3, North Anna Early Site Permit Application, Dominion Nuclear North Anna, LLC, U.S. Nuclear Regulatory Commission, Report ML042800292, 110 p.

Electric Power Research Institute (EPRI), US Department of Energy (DOE), and US Nuclear Regulatory Commission (NRC), 2012, Central and Eastern United States Seismic Source Characterization for Nuclear Facilities, NUREG-2115, EPRI, Palo Alto, CA.

Green, R.A., Obermeier, S.F., Olson, S.M., 2005, Engineering geologic and geotechnical analysis of paleoseismic shaking using liquefaction effects: field examples, Engineering Geology, v. 76, p. 263-293.

Green, R., Lasley, S., Carter, M.W., Munsey, J.W., Maurer, B W., Tuttle, M.P., 2015, Geotechnical aspects in the epicentral region of the 2011 Mw 5.8 Mineral, Virginia, earthquake, in Horton, J.W., Jr., Chapman, M.C., and Green, R.A., eds., The 2011 Mineral, Virginia, earthquake, and its significance for seismic hazards in eastern North America, Geological Society of America Special Paper 509. doi:10.1130/2015.2509(09)

Horton, J.W., Chapman, M.C., and Green, R.A., 2015, The 2011 Mineral, Virginia, earthquake, and its significance for seismic hazards in eastern North America-Overview and synthesis, *in* Horton, J. W., Jr., Chapman, M. C., and Green, R. A., eds., The 2011 Mineral, Virginia, earthquake, and its significance for seismic hazards in eastern North America, Geological Society of America Special Paper 509, p. 1-25.

Hough, S.E., 2012, Initial assessment of the intensity distribution of the 2011 Mw5.8 Mineral, Virginia, earthquake, Seismological Research Letters, v. 83, 649–657, https://doi.org/10.1785/0220110140.

Hughes, K.S., Hibbard, J.P., and Bohnenstiehl, D.R., 2015, Relict Paleozoic faults in the epicentral area of the August 23, 2011 central Virginia earthquake: Assessing the relationship between preexisting strain and modern seismicity, *in* Horton, J.W., Jr., Chapman, M.C., and Green, R.A., eds., The 2011 Mineral, Virginia, earthquake, and its significance for seismic hazards in eastern North America, Geological Society of America Special Paper 509, p. 331- 343.

Idriss, I.M., and Boulanger, R.W., 2004, Semi-empirical procedures for evaluating liquefaction potential during earthquakes, Proc., 11th International Conference on Soil Dynamics and Earthquake Engineering, and 3rd International Conference on Earthquake Geotechnical Engineering, D. Doolin et al., eds., Stallion Press, v. 1, p. 32-56.

Juang, C.H., Zhang, J., Khoshnevisan, S., and Gong, W., 2017, Probabilistic methods for assessing soil liquefaction and effect, Geo-Risk 2017: Keynote Lectures, American Society of Civil Engineers, p. 122-145, https://doi.org/10.1061/9780784480694.

Juang, C.H., and Jiang, T., 2000, Assessing probablistic methods for liquefaction potential evaluation, Soil Dynamics and Liquefaction 2000, GSP 107 (Proceedings GeoDenver), American Society of Civil Engineers, Reston, VA.

Kempthorne, D., and Myers, M.D., 2006, The Virginia Coastal Plain hydrogeologic framework, U.S. Geological Survey, Professional Paper 1731, 114 p.

Liang, P., and Forman, S.L., 2019, LDAC: An Excel-based program for luminescence equivalent dose and burial age calculations, Ancient TL, v. 37, p. 21-40.

L'Isle, G.D., 1718, Carte de Louisiane et du cours du Mississippi. [Paris] [Map] Retrieved from the Library of Congress, https://www.loc.gov/item/98685731/.

Mixon, R.B., Berquist, C.R., Jr., Newell, W.L., and Johnson, G.H., 1989, Geological map and generalized cross section of the Coastal Plain and adjacent parts of the Piedmont, Virginia, U.S. Geological Survey, Miscellaneous Investigations Series Map I-2033; scale 1:250,000.

Mixon, R.B., Pavlides, L., Powars, D.S., Froelich, A.J., et al., 2000, Geological map of the Fredericksburg 30’ x 60’ quadrangle, Virginia and Maryland, U.S. Geological Survey, Geological Investigations Series Map I-2607; scale 1:100,000.

Mueller, C.S., 2019, Earthquake catalogs for the USGS National Seismic Hazard maps, Seismological Research Letters, v. 90, n. 1, p. 251-261. https://doi.org/10.1785/0220170108

Obermeier, S.F., and McNulty, W.E., 1998, Paleoliquefaction evidence for seismic quiescence in central Virginia during late and middle Holocene time, EOS, Transactions of the American Geophysical Union, v. 79, no. 17, Spring Meeting Supplement, Abstract T41A-9.

Pazzaglia, F.J., Malenda, H.F., McGavick, M.L., Raup, C., Carter, M.W., Berti, C., Mahan, S., Nelson, M., Rittenour, T.M., Counts, R., Willenbring, J., Germanoski, D., Peters, S.C., and Holt, W.D., 2021, River terrace evidence of tectonic processes in the eastern North American Plate interior, South Anna River, Virginia: The Journal of Geology, v. 129, n. 5, University of Chicago, https://doi.org/10.1086/712636.

Petersen, M.D., Shumway, A.M., Powers, P.M., Field, E.H., et al., 2024, The 2023 U.S. 50-State National Seismic Hazard Model: Overview and implications, Earthquake Spectra, v. 40, n. 1, p. 5-88, doi: https://doi.org/10.1177/87552930231215428

Powars, D.S., Catchings, R.D., Horton, J.W., Jr., Schindler, S., and Pavich, M.J., 2015, Stafford fault system: 120 million year fault movement history of northern Virginia, *in* Horton, J.W., Jr., Chapman, M.C., and Green, R A., eds., The 2011 Mineral, Virginia, earthquake, and its significance for seismic hazards in eastern North America, Geological Society of America Special Paper 509, p. 407-431.

Pratt, T.L., Horton, J.W, Jr., Muñoz, J., Hough, S.E., Chapman, M.C., and Olgun, C.G., 2017, Amplification of earthquake ground motions in Washington, D.C., and implications for hazard assessments in central and eastern North America, Geophysical Research Letters, v. 44, https://doi.org/10.1002/2017GL075517.

Prescott, J.R., and Hutton, J.T., 1994, Cosmic ray contributions to dose rates for luminescence and ESR dating: Large depths and long-term time variations, Radiation Measurements, v. 23, p. 497-500.

Reimer, P.J., Austin, W E.N., Bard, E., Bayliss, A., et al., 2020, The IntCal20 northern hemisphere radiocarbon age calibration curve (0-55 cal kBP), Radiocarbon, v. 62, n. 4, p. 725-757, doi: 10.1017/RDC.2020.41

Robertson, P. K., 2010, Evaluation of flow liquefaction and liquefied strength using the CPT, Journal of Geotechnical and Geoenvironmental Engineering, v. 136, n. 6, p. 842-853.

Rukstales, K.S., and Petersen, M.D., 2019, Data release for 2018 update of the U.S. National Seismic Hazard Model: U.S. Geological Survey data release, https://doi.org/10.5066/P9WT5OVB.

Shaw, B.E., 2023, Magnitude and slip scaling relations for fault-based seismic hazard, Bulletin of the Seismological Society of America, v. 113, n. 3, p. 924-947, doi: https://doi.org/10.1785/0120220144.

Seed, H.B. and Idriss, I.M., 1971, Simplified procedure for evaluating soil liquefaction potential. Journal of the Soil Mechanics & Foundations Division (ASCE), v. 97 (SM9), p. 1249-1273.

Seed, H.B., and Idriss, I.M., 1982, Ground motions and soil liquefaction during earthquakes, Earthquake Engineering Research Institute, Berkley, 134 p.

Shumway, A.M., Petersen, M.D., Powers, P.M., Toro, G., et al., 2024, Earthquake rupture forecast model construction for the 2023 U.S. 50-State National Seismic Hazard Model update: Central and eastern U.S. fault-based source model, Seismological Research Letters, v. 95, p. 997-1029, doi: https://doi.org/10.1785/0220230294.

Sims, J.D., 1973, Earthquake-induced structures in sediments of Van Norman Lake, San Fernando California, Science, v. 182, p. 161-163.

Sims, J.D., 1975, Determining earthquake recurrence intervals from deformational structures in young lacustrine sediments, Tectonophysics, v. 29, p. 141–153. doi:10.1016/0040-1951(75)90139-0

Sims, J.D, 2012, Earthquake-induced load casts, pseudonodules, ball-and-pillow, and convolute lamination: additional deformation structures for paleoseismic studies, *in* Cox, R.T., Tuttle, M.P., Boyd, O.S., Locat, J., eds., Recent advances in North American paleoseismology and neotectonics east of the Rockies, Geological Society of America, Special Paper 493, p. 191–202. doi:10.1130/2012.2493(09)

Thompson Jobe, J.A., Hatem, A.E., Gold, R.D., DuRoss, C.B., et al., 2022, Revised earthquake geology inputs for the central and eastern United States and southeast Canada for the 2023 U.S. 50-State National Seismic Hazard Model, Seismological Research Letters, v. 93, n. 6, p. 3100-3120, doi: https://doi.org/10.1785/0220220162.

Tuttle, M., Law, T., Seeber, L., and Jacob, K., 1990, Liquefaction and ground failure in Ferland, Quebec, triggered by the 1988 Saguenay Earthquake, Canadian Geotechnical Journal, v. 27, p. 580-589.

Tuttle, M.P., and Hartleb R., 2012, Appendix E. Central and Eastern U.S. paleoliquefaction database, uncertainties associated with paleoliquefaction data, and guidance for seismic source characterization, *in* The Central and Eastern U.S. Seismic Source Characterization for Nuclear Facilities, Technical Report, EPRI, Palo Alto, CA, U.S. DOE, and U.S. NRC, 135 p. plus database, http://ceus-ssc.com/Report/AppendixE.html.

Tuttle, M.P., Wolf, L.W., Mayne, P.W., Dyer-Williams, K., and Lafferty, R.H., 2018, Guidance document: Conducting paleoliquefaction studies for earthquake source characterization, U.S. Nuclear Regulatory Agency, NUREG/CR-7238, 185 p, https://www.nrc.gov/docs/ML1801/ML18012A048.pdf.

Tuttle, M.P., Hartleb, R., Wolf, L., and Mayne, P.W., 2019, Paleoliquefaction studies and the evaluation of seismic hazard, Geosciences, v. 9, n. 7, 61 p. doi:10.3390/geosciences9070311.

Tuttle, M.P., Dyer-Williams, K., Carter, M.W., Forman, S.L., Tucker, K., Fuentes, Z., Velez, C., and Bauer, L.M., 2021, The liquefaction record of past earthquakes in the Central Virginia seismic zone, Eastern United States, Seismological Research Letters, v. 92, p. 3126-3144 plus electronic supplement. doi: https://doi.org/10.1785/0220200456.

Tuttle M. P., Dyer-Williams, K, and Tucker, K., 2023a, Paleoliquefaction studies of the Central Virginia seismic zone, U.S. Nuclear Regulatory Commission, RIL-2023-04, 70 p, https://www.nrc.gov/docs/ML2312/ML23124A197.pdf.

Tuttle, M. P., Dyer-Williams, K., and Tucker, K., 2023b, Improving estimates of the timing, locations, and magnitudes of paleoearthquakes in the Central Virginia seismic zone, Final Technical Report, Earthquake Hazard Program, U.S. Geological Survey award number G21AP10219, 36 p.

Uner, S., 2014, Seismogenic structures in Quaternary lacustrine deposits of Lake Van (eastern Turkey), Geologos, v. 20, p. 79–87, doi:10.2478/logos-2014-0011.

Virginia Division of Mineral Resources (DMR), 1993, Geologic map of Virginia, Virginia Division of Mineral Resources, scale 1:500,000.

Youd, T.L., and Idriss, I.M., 2001, Liquefaction resistance of soils: Summary report from the 1996 NCEER and 1998 NCEER/NSF workshops on evaluation of liquefaction resistance of soils, Journal of Geotechnical and Geoenvironmental Engineering, v. 127, n. 4, p. 297-313.

APPENDIX A STUDY SITES

Table A-1: Study Sites along Rivers in the CVSZ

Site	Latitude Longitude	Cutbank Exposure[1]	Liquefaction Feature[1, 2]	Weathering of Feature	Constraining Ages (yr B.P.)[1,3]
			Appomattox River		
AR1	37.3178 -78.4098	2.35 m high – loose sand layer at surface, overlying brown, micaceous, f-m sand fining upward to silt, underlain by mottled, silty, very fine sand and mottled silt; probe: same as above with thin (5-10 cm) sand layers; rock 1 m BWL	None	Not applicable	Modern AR1-OSL1 from base of upper sandy unit; ≤23,190 ± 1,525 AR1-OSL2 from base of lower silty unit
AR2	37.3063 -78.3956	2 m high – loose sand layer at surface, underlain by reddish brown, silt followed by interbedded grayish silt & brownish sand (3-5 cm); micaceous	None	Not applicable	Modern AR1-OSL1 from upper sandy unit; ≤23,190 ± 1,525 AR1-OSL2 from lower silty unit
AR3	37.4433 -78.1759	3 m high – loose sand layer at surface, over-lying reddish brown, micaceous silty fine sand, underlain by mottled silty sand, silt, clayey silt, & sandy silt with lines of pebbles & lenses of pebbly coarse sand; probe: same as above w/ several thin layers of sand to 1.25 m BWL	None	Not applicable	≤260 AR3-C1 from base of upper sandy sand; 2,570 ± 130 AR3-OSL2 from mottled silt; >46,390 AR3-OSL3 from pebble lense within lower portion sandy silt
AR4	37.4487 -78.1266	3 m high – sand under-lain by mottled very fine sandy silt followed by mottled interbedded silt & sand; probe: same as above; pebbly sand at 1 m BWL	None	Not applicable	>53,940 AR4-OSL1 from sand layer in interbedded silt & sand near base of cutbank
AR5	37.4845 -77.9629	3 m high – lower 1 m exposed; yellowish-red, very fine sandy silt, micaceous, with pebbles & cobbles; probe: sandy silt underlain by sand at 1.4+ m BWL	C2: Three dikes, 10, 1, and 0.5 cm wide, intruding cracks; extend to 0.6 m AWL or 2.4 m BS	Bioturbated & mottled, iron staining along lower margins of dikes	2,560-3,615 >2,560 AR8-OSL1; <3,615 AR8-OSL2; <26,525 ± 2,195 AR5-OSL1

AR6	37.4815 -77.9531	2.5 m high – lower 2 m exposed; mottled, very fine sandy silt; probe: similar to above except for layers of sand at 0.33-0.36, 1.30-1.33, & 1.45-1.60 m BWL	C2: One dike – 2 cm wide, branches upward and extends to at least 0.6 m AWL or 1.9 m BS	Bioturbated & mottled, especially upper part of dikes	2,560-3,615 >2,560 AR8-OSL1; <3,615 AR8-OSL2
AR7	37.4794 -77.9474	3 m high – lower 2.5 m exposed; mottled, fining upward silty sand; probe: silty sand underlain by sand at 1.2-1.5+ m BWL	C1: Large, 12 cm wide, dike low in cutbank, feeds small diapir & two dikes 2 cm wide that extend to 0.65 m AWL or 2.35 m BS	Bioturbated & mottled, especially upper part of dike; iron staining along lower margins	2,560-3,615 >2,560 AR8-OSL1; <3,615 AR8-OSL2; <24,650 ± 995 AR7-OSL1
AR8	37.4783 -77.9193	3.8 m high – lower 2.3 m exposed; silty very fine sand underlain by silt loam followed by mottled silt with manganese nodules & mottled silty very fine sand; probe: same as above to 0.82 m, sand to 0.94 m, followed by silty very fine sand to 1.5 m BWL	C1: Six dikes – 10, 8, 7, 3, 2, & 2 cm wide, extend to 2.04 m AWL or 1.76 m BS; discontinuous dikes continue to 2.25 m AWL or 1.55 m BS; krotovina casts injected by sand, become dikes higher in section; krotovi-na crosscut by younger dikes	Older gener-ation dikes – iron stained, mottled, & bioturbated especially margins; younger generation dikes – un-weathered	Older generation 2,560-3,615 >2,560 AR8-OSL1; <3,615 AR8-OSL2; younger generation-probably historic <270
AR100	37.4722 -78.0167	3 m high – drab silt underlain by reddish, silty sand followed by bioturbated & mottled silt & silty sand with Fe & Mn staining and few nodules, pebbly near base of unit, underlain by loose, fine-medium sand to pebbly medium-coarse sand; rock outcrop at WL	C1: Seven dikes, 3, 3, 3, 3, 2, 1, & 0.5 cm wide, and one sill, 5 cm thick; several dikes extend to 1 m AWL or 2 m BS into reddish, silty sand; sill intrudes along base of reddish, silty sand; dikes branch upward from sill and extend to 2 m AWL or 1 m BS pinching out in drab silt	Dikes & sill bioturbated and mottled	<74,340 AR100-OSL1 from drab silt provides maxi-mum age con-straint for dikes higher in cutbank; <86,440: AR100-OSL3 from mottled silty sand provides maximum age constraint for dikes & sills lower in cutbank; also provides min-imum age con-straint for source sand of dikes
AR101	37.4843 -78.0194	3.4 m high – drab silt underlain by reddish, silty sand followed by bioturbated & mottled silty sand with Fe and Mn staining	C1: Four dikes, 8.5, 6, 3, & 3 cm wide, & one sill, 3 cm thick; sill intruded within mottled silty sand; three dikes branch upward from sill, two dikes extend into reddish, silty sand &	Dikes biotur-bated and mottled; finer portions of sill gleyed, coarser portion Fe-stained	<77,540 AR100-OSL2 from reddish, silty sand provides maximum age constraint for dikes that pinch out in this unit <86,440

			pinch at 1.4 m AWL or 2 m BS		AR100-OSL3 from mottled silty sand provides maximum age constraint for dikes and sills lower in cutbank
AR102	37.4914 -78.0125	2.8 m high – brown, silty sand (loam) underlain by drab silt followed by mottled silty sand with Fe & Mn staining which becomes pebbly sand near base of cutbank	C2: Two dikes, 4 & 3 cm wide; both crosscut mottled silty sand & extend into drab silt, pinching at 1.1 and 1.2 m AWL or 1.7 and 1.6 m BS	Bioturbated & mottled	<77,540 AR100-OSL2 from reddish, silty sand provides maximum age constraint for sand dikes
AR103	37.4952 -77.9974	3.2 m high – upper 0.5 m covered by vegetation & roots; drab silt underlain by reddish, silty sand	C3: One possible dike, 3.5 cm wide; crosscuts reddish, silty sand, extends into drab silt, pinching at 2 m AWL or 1.2 m BS	Not noted	<74,340 AR100-OSL1 from drab silt provides maxi-mum age con-straint for dikes that terminate higher in cutbank
AR104	37.4862 -77.9859	3.9 m high – upper 1-2 m covered by vegetation & slump; mottled silt underlain by mottled, interbedded sandy silt & sand; layers of pebbly sand and coarse-medium sand towards bottom of cutbank	C2: Two dikes, 5 & 2.5 cm wide; one originates in pebbly sand, crosscuts inter-bedded sandy silt & sand, extends into mottled silt, pinching at 1.9 m AWL or 2 m BS; slump covers upper part of second dike	Bioturbated & mottled	<86,440 AR100-OSL3 from mottled silty sand provides maximum age constraint
AR105	37.4559 -78.0924	3 m high – upper 1.5 m covered by vegetation; reddish brown, silt underlain by reddish, silty sand; probe: same as above to cemented layer at 0.5 m BWL; finer below	C3: Two possible dikes, 2 & 2 cm wide; both intrude reddish, silty sand; one dike branches upward & pinches at contact with over-lying silt at 1.1 m AWL or 1.9 m BS; other dike pinches within silty sand	Bioturbated & mottled	<19,420 ± 695 AR106-OSL1 from reddish, sand provides maximum age constraint for dikes
AR106	37.4570 -78.0892	3 m high – upper 1.5-2 m covered by vegetation; mottled silty sand underlain by reddish, medium-fine sand, micaceous; probe: loose sand to 0.25 m BWL, then difficult to push probe	C2: Two dikes, 3 & 1 cm wide; both dikes originate in reddish, medium-fine sand, widen below contact with overlying mottled silty sand, branch into multiple dikes that extend into	Bioturbated & mottled	<19,420 ± 695 AR106-OSL1 from reddish, sand provides maximum age constraint for dikes

			overlying silty sand, pinching at 0.9-1 m AWL or 2.1-2 m BS		
AR107	37.4523 -78.0746	3 m high – upper 1.5 m covered by vegetation; reddish silt with small amount of very fine sand, few lines of pebbles, & sand layer towards bottom of cutbank; probe: cemented pebbly sand BWL	C2: Two dikes, 2 & 1 cm wide, cross-cut reddish silt & sandy interbed, branch upward, & pinch at 0.6 m AWL or 2.4 m BS and 0.3 m AWL or 2.7 m BS; dikes probably originate in pebbly sand BWL	Bioturbated & mottled	<19,420 ± 695 AR106-OSL1 from reddish, sand provides maximum age constraint for dikes
AR108a	37.4717 -78.0508	3 m high – upper 1.5 m covered by vegetation; reddish silty sand followed by bioturbated & mottled silty sand with Fe & Mn staining; layer of gray, silty very fine sand at WL	C1: Three dikes, 2.5, 2, & 0.5 cm wide; two larger dikes originate in silty, very fine sand layer near base of cutbank, crosscut mottled, silty sand & reddish, silty sand, branching upward & pinching at 1.4 m AWL or 1.6 m BS	Bioturbated & mottled	<18,960 ± 880 AR108b-OSL1 from reddish brown silty sand and adjacent to dike tip provides maximum age constraint
AR108b	37.4721 -78.0501	3 m – drab silt underlain by reddish brown and reddish, silty sand followed by bioturbated & mottled silty sand with Fe & Mn staining	C1: Two dikes, 12 & 6 cm wide; crosscut mottled, silty sand, & reddish, silty sand, branch upward, and pinch at 1.3 m and 1.45 m AWL or 1.7 m and 1.55 m BS; dikes composed of silty, very fine sand similar to source layer observed at nearby OSL108a	Bioturbated & mottled	<18,960 ± 880 AR108b-OSL1 from reddish brown silty sand provides maximum age constraint
AR109	37.4717 -78.0289	3 m high – upper 1.5 m covered by vegetation & colluvium; mottled silty sand; probe: same as above	C3: Two possible dikes, 3 & 2 cm wide; crosscut mottled, silty sand, pinch at 0.7 m & 0.8 m AWL or 2.3 & 2.2 m BS	Bioturbated & mottled; difficult to track	Probably similar in age to dikes at AR108
AR110	37.4768 -77.9165	3.7 m high – upper 1.4 m covered by vegetation; loose, silty, medium-fine sand underlain by reddish, silty sand, followed by bioturbated very fine	C1-2: Three dikes, 7, 4, and 2.5 cm wide; crosscut bioturbated and mottled, silty sand & sandy silt, branching upward; one dike	Bioturbated & mottled	<13,055 ± 620 AR110-OSL2 from reddish, silty sand and adjacent to dike tips provides maximum age

		sandy silt and silty sand with Fe & Mn staining and large krotovina casts; probe: medium-fine sand underlain by rock at 0.3 m BWL	extends into reddish, silty sand, becomes discontinuous and pinches at 2.25 m AWL or 1.45 m BS; two other dikes pinch in mottled sandy silt		constraint; other dikes probably similar in age
AR111	37.4554 -77.8782	3 m high – upper 2 m covered by vegetation; bioturbated & mottled silt; probe: similar to above, underlain by sand 0.5-0.76 m BWL, cemented	C2: One dike, 2 cm wide; intrudes mottled silt, branches laterally & upward, and pinches at 0.4 m AWL or 2.6 m BS	Bioturbated & mottled; lower 10 cm gleyed	Correlation uncertain
AR112	37.4535 -78.1480	2.5 m high – upper 1 m covered by vegetation; reddish sand underlain by mottled silty clay with pebble lines; probe: similar to above, underlain by sand 0.45-0.7 m BWL, followed by rock	C3: Two possible dikes: 1.5 & 1 cm wide; subvertical near base of cutbank, branch and become low-angle dikes upsection; pinch at 0.7 and 0.4 m AWL or 1.8 and 2.1 m BS	Gleyed; difficult to trace	<19,160 ± 840 AR112-OSL1 from mottled, silty clay and adjacent to dike tip provides maximum age constraint
AR113	37.4559 -78.1462	3 m high – upper 1 m covered by vegetation; reddish sand underlain by mottled silty sand	C3: Two possible dikes: largest up to 9 cm wide, branches upward & terminates at 0.95 m AWL or 2.05 m BS; 1 cm wide dike w/ lateral continuity extends upward from kroto-vina cast, pinches within silty sand	Bioturbated margins; gleyed	<19,160 ± 840 AR112-OSL1 probably provides maximum age constraint
AR114	37.4563 -78.1434	3 m high – upper 0.5 m loose sand, underlain by 0.3 m of reddish sand followed by mottled, silty sand & interbed-ded silt and sand, lower 0.3 m Fe & Mn stained; probe: similar to above, with sand from 0.1-1 m BWL, followed by rock	C2: Three dikes, 2.5, 1.5, 1 cm wide, one dike originates below water level, other two originate in sand layers within interbedded silt & sand unit; two dikes pinch at 0.6 m AWL or 2.4 m BS in another sand layer	Bioturbated margins; gleyed	<28,485 ± 1,175 AR115-OSL1 from mottled, silty sand with Fe & Mn staining provides maximum age constraint
AR115	37.4546 -78.1318	3.8 m high – upper 0.5 m covered by vegeta-tion; 1.9 m reddish sand underlain by mottled silty sand, lower 0.3 m Fe & Mn stained; probe: similar	C3: One possible dike: 2 cm wide; intrudes mottled silty sand and pinches at 0.56 m AWL or 3.24 m BS	Bioturbated & mottled	<28,485 ± 1,175 AR115-OSL1 from mottled, silty sand with Fe & Mn staining and adjacent to dike tip provides

		to above, underlain by sand from 0.45-1 m BWL, followed by rock			maximum age constraint
AR116	37.4488 -78.1268	3 m high – upper 0.5 m covered by vegetation; reddish sand underlain by mottled silty sand, lower 0.5 m Fe & Mn stained	C3: One possible dike: 1 cm wide; intrudes mottled silty sand & pinches 0.7 cm AWL or 2.3 m BS; also, two smaller discontinu-ous dikes; all within a 10 cm wide zone	Bioturbated margins; gleyed	<4,100 ± 135 AR117-OSL1 from mottled, silty sand probably provides maximum age constraint
AR117	37.4495 -78.1055	4 m high – upper 2.75 m covered by vegeta-tion; brownish silt with crumb structure, likely soil, coarsening down-ward to mottled silty sand, lower 0.5 m Fe & Mn stained; probe: similar to above, underlain by sand from 0.3-1.45+ m BWL	C2: Two dikes: 4 & 4 cm wide, intrude silty sand, branch upward, & terminate at 0.8 m AWL or 3.2 m BS at base of likely soil	Bioturbated & mottled	<4,100 ± 135 AR117-OSL1 from mottled, silty sand and adjacent to dike terminations at base of likely soil provides maximum age constraint
AR118	37.4430 -78.0973	3 m high – upper 1 m drab silt underlain by reddish sand; followed by mottled, silty clay, lower 0.3 m Fe & Mn stained	C2: Three dikes – 4.5, 4, and 1.5; intrude silty clay and branch upward; two dikes terminate within silty clay; third dike extends into reddish sand and pinches at 0.8 m AWL or 2.2 m BS	Bioturbated margins; gleyed	<19,420 ± 695 AR106-OSL1 from reddish, sand provides maximum age constraint for dikes
Mattaponi River					
MR200	37.8765 -77.1492	1 m high – mottled, silt, underlain by interbed-ded white sand with pebbles & gray silt; pebbles at water level	None	Not applicable	≤470 MR200-C1 about 0.75 m BS from silty sand
MR201	37.8390 -77.1229	6 m high – lower 4 m exposed; sand underlain by bioturbated & mottled silty sand followed by brownish clayey silt with subvert-tical joints; probe: same as above, then sand 0.5-1+ m BWL	None	Not applicable	≤37,671 MR201-W1 4.1 m BS from mottled silty sand

MR202	37.8309 -77.1224	6 m high – lower 2 m exposed; pebbly sand underlain by bioturbated & mottled silty sand followed by brownish clayey silt with sub-vertical joints; probe: same as above, then sand 0.25+ m BWL	None: root casts & joints filled with loose silt and sand	Not applicable	37,671 MR201-W1 4.1 m BS from mottled silty sand
		Nottoway River			
NR1	36.8708 -77.4575	4 m high – reddish brown silt loam, underlain by reddish clayey silt followed by coarse-medium sand	None	Not applicable	140-170 NR1-OSL1 from clayey silt; >39,940 NR1-OSL2 from coarse-medium sand
		Pamunkey River			
PR2	37.7972 -77.3603	4-4.5 m high – upper 2.5 m vegetated, lower 1.5 m exposed; reddish, silty very fine sand underlain by mottled, very fine sandy silt, followed by mottled silt; probe: silt with sand layers at 80-85 cm & 128-132 cm BWL	C2: Four sand dikes – 2.7-7.3 cm wide, extend to 95 cm AWL; tabular, branch & narrow up-section	Upper part of dikes biotur-bated & iron stained	<8,075 ± 305 PR2-OSL1 from mottled sandy silt, level of dike tips; ≤16,345 ± 675 PR2-OSL2 silty sand near base of cutbank
PR5	37.7893 -77.3297	4-5 m high – silty fine sand with pebbles underlain by white sand followed by mottled clayey silt	None	Not applicable	≤4,618-4,818 PR5-C2 from organic sediment in lower part of white sand
PR100	37.7218 -77.2731	3.5 m high – only lower 0.6 m exposed; mottled silt	C2: Two sand dikes – 4 cm & 0.5 cm wide; silty fine sand; extend to 0.2 and 0.4 m AWL or 3.3 and 3.1 m BS	Upper part of dikes some-what biotur-bated	<1,990 ± 100 PR100-OSL1 3.3 m BS from mottled silt level with lower dike tips
PR201	37.6591 -77.1723	1.85 m high – fairly well-exposed; upper unit of reddish pebbly sand fines upward to yellowish sand; underlain by mottled, reddish silt with manganese nodules; probe: silt with thin layers of sand	None	Not applicable	≤13,065 ± 645 PR201-OSL2 1 m BS from base of upper sandy unit; ≤14,590 ± 790 PR201-OSL1 1.6 m BS from reddish silt
		Rapidan River			
RnR1	38.3186 -78.0359	4 m high – lower 1.5 m well exposed; inter-bedded iron-stained sand & silt underlain by gray silt with rock	C2: Soft-sediment deformation – pseudonodules or rounded sandy masses, diapirs and	Iron stained	215-310 RnR1-OSL1 & OSL2 bracket age of SSDs; 142-1818

		fragments followed by mottled very fine sandy silt; probe: sandy silt to rock at 0.75 m	flames		RnR1-C1 & C2 bracket age of SSDs
RnR2	38.3220 -78.0342	2 m high – lower 1 m exposed; loose & unweathered, interbed-ded sand & silty sand	None	Not applicable	Modern RnR2-C1 from unweathered silty sand
RnR3	38.3469 -77.9761	3 m high – lower 1.5 m exposed; reddish silt with thin layers of sand overlying bioturbated & mottled silt & sand; probe: interbedded silt & sand; rock at 0.5 m BWL	C2: Sand dike – 1 cm, extends 0.25 m AWL, and sandy domains in bioturbated and mottled silt; flames of sand at 0.4 m AWL	Dike, gleyed; flames, iron stained	215-310 probably formed at same time as SSDs at RnR1 ≤330 ± 15 RnR3-OSL1 provides max age constraint for dike & flames
Rivanna River-Stigger Creek					
RR-SC2	37.9087 -78.2884	4.7 m high – upper 2.5 m covered by vegetation, lower 2.2 m well exposed; reddish silt with lenses of cobbles and pebbles, underlain by somewhat mottled silty fine sand grading downward to mottled silty medium-fine sand, followed by cobbly, pebbly sand	C1: Four dikes – 2, 2, 1, 1 cm wide originate in cobbly, pebbly sand & medium-fine sand, crosscut silty fine sand, branch upward and pinch at contact with overlying reddish silt; one dike extends into overlying silt & pinches at 1.8 m AWL or 2.9 m BS	Bioturbated & mottled	<12,030 ± 525 RR-SC2-OSL1 near dike tip provides max constraining age; 24,140 ± 1105 RR-SC2-OSL 3 from source layer of dikes
South Anna River					
SoAR7	37.9158 -77.9307	2 m high – upper 1 m somewhat vegetated, lower 1 m well exposed; interbedded silt and sand underlain by mottled clayey silt; probe: clayey silt, underlain by 0.9 m of sand, followed by silt to 1.5 m BWL	C2: Sand dikes – 1 to 1.5 cm wide, branch upward; extends to 1 m BS or 1 m AWL	Mottling in dikes	<5,891 SoAR7-C4 from root cast in mottled clay silt crosscut by dikes; <9,015 ± 310 SoAR7-OSL1 from mottled clayey silt
SoAR10a	37.7760 -77.8219	2 m high – upper 1 m vegetated, lower 1 m well exposed; bioturbated and mottled, sandy silt	C2: Sand dike – 4 cm wide, branches upward; extends to 1.7 m BS or 30 cm AWL	Some biotur-bation and mottling	<8,696 SoAR10a-C1 from mottled sandy silt, 20 cm below dike tip
SoAR10b	37.7761 -77.8217	2.5 m high – upper 1.25 m vegetated, lower 1.25 m well exposed; drab silt underlain by mottled silt & sand, with hint of layering, followed by interbedded silty sand &	C2: Silty sand dikes – 4 cm, 2 cm, 2 cm, 1 cm wide, branch upward; two dikes extend to 1.45 m BS or 1.05 m AWL, discontinuous to 1.25	Some biotur-bation and mottling in upper part of dikes	<8,696 SoAR10a-C1 from mottled sandy silt, 20 cm below dike tip; <13,800 ± 530 SoAR10b-OSL2

		silt; probe: same above to 50 cm BWL, followed by coarser sand for 10 cm to rock	m BS; two other dikes intrude polygonal cracks		from interbedded sand & silt, 98 cm below dike tips

[1] Abbreviations: AWL = above water level; BWL = below water level; BS = below ground surface/top of cutbank.

[2] Confidence (C): 1 = high; 2 = medium; 3 = low. Features with C values of 1 or 2 are shown in Figures 1-1 and 5-2.

[3] Calibrated C14 and OSL ages in years B.P. or before A.D. 1950; < = after, > = before.

APPENDIX B   DATING RESULTS

Table B-1: Radiocarbon Dating of Organic Samples from the CVSZ (this study and Tuttle et al., 2023a,b)

Site-Sample Lab No.[1]	$^{13}C/^{12}C$ Ratio	Conventional ^{14}C Age Yr B.P.[2]	Calibrated Age Yr B.P.[3] 1-sigma	Calibrated Calendar Date[3] 1-sigma	Prob. %	Calibrated Age Yr B.P.[3] 2-sigma	Calibrated Calendar Date[3] 2-sigma	Prob. %	Sample Description[4]
Appomattox River									
AR3-C1 BA633122	-26.5	120 ± 30	29-47 56-120 124-142 222-233 238-260	AD 1921-1903 AD 1894-1830 AD 1826-1808 AD 1728-1717 AD 1712-1690	9.2 34.3 8.4 5.3 11	10-151 186-198 210-270	AD 1940-1799 AD 1764-1752 AD 1740-1680	67.2 2.4 25.8	Charred material; from silty fine sand ~3 cm above buried soil; 62 cm BS
Mattaponi River									
MR200-C1 BA609013	-25.9	350 ± 30	322-377 428-470	AD 1628-1573 AD 1522-1480	38 30.2	315-411 420-490	AD 1635-1539 AD 1530-1460	55.4 40	Charred material from silty very fine sand; collected 75 cm BS or 25 cm AWL
MR201-W1 BA609014	-21.6	32,940 ± 230	36961-37671	BC 35012-35722	68.2	36679-38474	BC 36525-34730	95.4	Flat piece of wood from mottled silty sand; collected 10 cm above clayey silt; 4.1 m BS or 1.9 m AWL
Pamunkey River									
PR5-C2 BA647238	-24.6	4,150 ± 30	4618-4726 4750-4765 4788-4818	2669-2777 BC 2801-2816 BC 2839-2869 BC	48.3 6.5 13.4	4575-4825	2626-2876 BC	95.4	Organic sediment; from basal portion of white sand; 1.5 m AWL & 3.5 m BS; 15 cm above mottled clayey silt
Rapidan River									
RnR1-C1 BA609015	-24.3	1,850 ± 30	1714-1750 1760-1792 1810-1818	AD 236-200 AD 190-158 AD 140-132	35.4 26 6.8	1644-1652 1702-1830	AD 306-298 AD 248-120	1.1 94.3	Charred material; from mottled very fine sandy silt 35 cm below SSD; 3.55 m BS or 45 cm AWL

Site-Sample Lab No.[1]	$^{13}C/^{12}C$ Ratio	Conventional ^{14}C Age Yr B.P.[2]	Calibrated Age Yr B.P.[3] 1-sigma	Calibrated Calendar Date[3] 1-sigma	Prob. %	Calibrated Age Yr B.P.[3] 2-sigma	Calibrated Calendar Date[3] 2-sigma	Prob. %	Sample Description[4]
RnR1-C2 BA609016	-25.4	170 ± 30	Post 0-28 142-154 168-222 260-282	Post AD 1950-1922 AD 1808-1796 AD 1782-1728 AD 1690-1668	16.1 6.5 32.6 13	Post 0-43 60-118 135-230 250-290	Post AD 1950-1907 AD 1890-1832 AD 1815-1720 AD 1700-1660	19.5 12.5 46.1 17.4	Charred material; from mottled sand layer within interbedded sand & silt unit 30 cm above SSD; 3.08 m BS or 92 cm AWL
RnR2-C1 BA609017	-24.6	100.88 ± 0.38 pMC	-5 to -6	AD 1955-1954	68.2	-5 to -6	AD 1955-1954	95.4	Charred material; large chunk with rounded corners; from un-weathered silty sand; collected 60 cm AWL
South Anna River									
SOAR7-C4 BA647240	-23.7	5,030 ± 30	5722-5760 5815-5891	BC 3773-3811 BC 3866-3942	21.8 46.4	5661-5694 5707-5897	BC 3712-3745 BC 3758-3948	7.6 87.8	Organic sediment; from root cast in mottled clayey silt; 1.5 m BS
SOAR10a-C1 BA647241	-23.4	7,860 ± 30	8592-8649 8673-8696	BC 6643-6700 BC 6724-6747	56 12.2	8549-8575 8585-8772	BC 6600-6626 BC 6636-6823	3.9 91.5	Organic sediment; from mottled very fine sandy silt; 1.8 m BS; 20 cm below dike tip

[1] BA stands for Beta Analytic, Inc.

[2] Conventional radiocarbon ages in years B.P. or before present (1950) determined by Beta Analytic, Inc. Errors represent 1 standard deviation statistics or 68% probability.

[3] Calibrated age ranges and calendar dates as determined by Beta Analytic, Inc., using the high probability density range method (Bronk Ramsey, 2009) and INTCAL20 (Reimer et al., 2020). 1-sigma error ranges represent 68.2% probability and 2-sigma ranges represent 95.4% probability.

[4] Abbreviations: AWL – above water level; BS – below ground surface/top of cutbank.

Table B-2: Radiocarbon Dating of Organic Samples from the CVSZ Collected During Prior Study (Tuttle et al., 2021)

Site-Sample Lab No.[1]	$^{13}C/^{12}C$ Ratio	Conventional ^{14}C Age Yr B.P.[2]	Calibrated Age Yr B.P.[3] 1-sigma	Calibrated Calendar Date[3] 1-sigma	Calibrated Age Yr B.P.[3] 2-sigma	Calibrated Calendar Date[3] 2-sigma	Sample Description[4]
James River							
JR1-C2 BA414596	-28.6	130 ± 30	Post 0 15-40 60-150 190-195 215-230 240-270	Post AD 1950 AD 1935-1910 AD 1890-1800 AD 1760-1755 AD 1735-1720 AD 1710-1680	Post 0-150 170-280	Post 1950-AD 1800 AD 1780-1670	Plant material; from leaf mat 22 cm below dike base & 10 cm awl
Mattaponi River							
MR102-C1 BA546852	-25.6	2490 ± 30	2495-2597 2611-2638 2683-2711	BC 546-648 BC 662-689 BC 734-762	2459-2730	510-781 BC	Charred material; angular piece collected from sand ~50 cm awl & 66 cm below silt/ sand contact; sand possible source of dikes at nearby sites
MR104-C1 BA547638	-24.8	6140 ± 30	6958-7028 7057-7068 7112-7155	BC 5009-5079 BC 5108-5119 BC 5163-5206	6951-7158	5002-5209 BC	Charred material; small angular piece collected from sand ~55 cm awl or 15 cm below mottled sandy silt/sand contact; sand possible source of dikes along lower river
Pamunkey River							
PR5-C1 BA414591	-26.0	4800 ± 30	5485-5525 5580-5590	BC 3535-3575 BC 3630-3640	5475-5550 5575-5595	BC 3525-3600 BC 3625-3645	Charred material; from mottled silt 25 cm AWL
PR6-W1 BA414592	-29.7	270 ± 30	295-310	AD 1655-1640	155-165 285-320 375-430	AD 1795-1785 AD 1665-1630 AD 1575-1520	Plant material; from leaf layer at water level

Site-Sample Lab No.[1]	$^{13}C/^{12}C$ Ratio	Conventional ^{14}C Age Yr B.P.[2]	Calibrated Age Yr B.P.[3] 1-sigma	Calibrated Calendar Date[3] 1-sigma	Calibrated Age Yr B.P.[3] 2-sigma	Calibrated Calendar Date[3] 2-sigma	Sample Description[4]
PR101-C1 BA547635	-27.1	2860 ± 30	2925-3007 3013-3032	BC 976-1058 BC 1064-1083	2878-3067	929-1118 BC	Charred material; small angular piece collected ~75 cm awl or 225 cm BS from mottled sandy silt & silt intruded by diapirs and dike
PR106-C1 BA547636	-25.7	5990 ± 30	6789-6860 6870-6881	BC 4840-4911 BC 4921-4932	6741-6907	BC 4792-4958	Charred material; small angular piece collected 23 cm awl or 152 cm BS from mottled silt intruded by dikes
South Anna River							
SoAR100-C1 BA414599	-26.3	3930 ± 30	4360-4365 4405-4420	BC 2410-2415 BC 2455-2470	4290-4435	BC 2340-2485	Plant material; from sandy unit 125 cm BWL

[1] BA stands for Beta Analytic, Inc.

[2] Conventional radiocarbon ages in years B.P. or before present (1950) determined by Beta Analytic, Inc. Errors represent 1 standard deviation statistics or 68% probability.

[3] Calibrated age ranges and calendar dates as determined by Beta Analytic, Inc., using the Pretoria procedure (Talma and Vogel, 1993; Vogel et al., 1993) or the high probability density range method (Bronk Ramsey, 2009) and INTCAL20 (Reimer et al., 2020). 1-sigma error ranges represent 68.2% probability and 2-sigma ranges represent 95.4% probability.

[4] Abbreviations: AWL – above water level; BWL – below water level; BS – below ground surface/top of cutbank.

Table B-3: Optically-Stimulated Luminescence Dating of Quartz Grains from Sediment in the CVSZ (this study)

Site-Sample Lab No. Depth (m)	Aliquots[a]	Grain Size (µm)	Equivalent Dose (De) (Gy)[b]	Over-dispersion (%)[c]	U (ppm)[d]	Th (ppm)[d]	K2O (%)[d]	Rb (ppm)	H20 (%)	Cosmic Dose Rate (mGray/yr)[e]	Dose Rate (mGray/yr)	OSL Age (Yr)[f]	OSL Age Yr. B.P.[g]	Sample Description
Appomattox River														
AR100-OSL1 BG5814 1.00	10/10	150-250	>160	NA	2.59 ± 0.01	6.62 ± 0.01	1.67 ± 0.01	61.3 ± 0.1	20 ± 3	0.185 ± 0.018	2.15 ± 0.06	>74,400	>74,340	Drab, silt; adjacent to dike tip
AR100-OSL2 BG5813 1.30	8/8	150-250	>160	NA	2.30 ± 0.01	6.37 ± 0.01	1.65 ± 0.01	52.8 ± 0.1	20 ± 3	0.182 ± 0.018	2.06 ± 0.05	>77,600	>77,540	Reddish, silty sand; crosscut by dikes
AR100-OSL3 BG5812 2.45	10/10	250-355	>160	NA	2.24 ± 0.01	3.03 ± 0.01	1.78 ± 0.01	43.0 ± 0.1	20 ± 3	0.161 ± 0.016	1.85 ± 0.05	>86,500	>86,440	Mottled, silty sand with Mn nodules; above source sand
AR106-OSL1 BG5810 2.40	20/20	250-355	38.89 ± 1.14	11 ± 2	2.17 ± 0.01	5.87 ± 0.01	1.74 ±0.01	56.7 ± 0.1	20 ± 3	0.161 ± 0.016	1.99 ± 0.05	19,480 ± 695	19,420 ± 695	Mottled, medium-fine sand; crosscut by dikes
AR108B-OSL1 BG5811 1.57	20/20	150-250	45.28 ± 1.67	15 ± 3	3.20 ± 0.01	8.62 ± 0.01	1.68 ±0.01	83.4 ± 0.1	20 ± 3	0.177 ± 0.018	2.38 ± 0.07	19,020 ± 880	18,960 ± 880	Reddish brown, silty sand; adjacent to dike tip
AR110-OSL1 BG5815 1.40	19/20	250-355	23.90 ± 0.74	12 ± 3	1.53 ± 0.01	3.92 ± 0.01	1.70 ± 0.01	52.6 ± 0.1	20 ± 3	0.180 ± 0.018	1.76 ± 0.08	13,550 ± 740	13,490 ± 740	Tan, medium-fine sand; above dike tips
AR110-OSL2 BG5816 1.50	20/20	250-355	24.14 ± 0.38	5 ± 1	1.84 ± 0.01	4.43 ± 0.01	1.69 ± 0.01	55.9 ± 0.1	20 ± 3	0.178 ± 0.018	1.84 ± 0.08	13,115 ± 620	13,055 ± 620	Reddish, silty sand; adjacent to dike tips
AR110-OSL3 BG5817 2.40	20/20	250-355	33.35 ± 0.70	7 ± 2	2.50 ± 0.01	6.53 ± 0.01	1.82 ± 0.01	73.7 ± 0.1	20 ± 3	0.161 ± 0.016	2.14 ± 0.06	15,575 ± 550	15,515 ± 550	Bioturbated and mottled, sandy silt
AR112-OSL1 BG5809 1.84	19/20	150-250	42.88 ± 1.45	14 ± 3	3.05 ± 0.01	8.21 ± 0.01	1.54 ± 0.01	69.5 ± 0.1	20 ± 3	0.172 ± 0.017	2.23 ± 0.06	19,220 ± 840	19,160 ± 840	Mottled, silty clay; near dike tip

Site-Sample Lab No. Depth (m)	Aliquots[a]	Grain Size (µm)	Equivalent Dose (De) (Gy)[b]	Over-dispersion (%)[c]	U (ppm)[d]	Th (ppm)[d]	K2O (%)[d]	Rb (ppm)	H20 (%)	Cosmic Dose Rate (mGray/yr)[e]	Dose Rate (mGray/yr)	OSL Age (Yr)[f]	OSL Age Yr. B.P. [g]	Sample Description
AR115-OSL1 BG5818 3.28	26/30	150-250	61.39 ± 1.84	13 ± 2	2.57 ± 0.01	7.45 ± 0.01	1.66 ± 0.01	67.1 ± 0.1	20 ± 3	0.147 ± 0.015	2.15 ± 0.06	28,545 ± 1,175	28,485 ± 1,175	Mottled, silty sand; adjacent to dike tip
AR117-OSL1 BG5819 3.24	24/24	150-250	10.80 ± 0.21	4 ± 1	3.76 ± 0.01	9.22 ± 0.01	1.83 ± 0.01	83.4 ± 0.1	20 ± 3	0.148 ± 0.015	2.59 ± 0.07	4,160 ± 135	4,100 ± 135	Mottled, silty sand; adjacent to dike tip
Nottoway River														
NR1-OSL1 BG5826 2.40	19/20	150-250	0.74 ± 0.04	22 ± 4	4.26 ± 0.01	11.75 ± 0.01	2.44 ± 0.01	108.5 ± 0.1	20 ± 3	0.160 ± 0.016	3.24 ± 0.09	215 ± 15	155 ± 15	Reddish, clayey silt
NR1-OSL2 BG5827 2.90	15/15	500-710	>124	NC	1.82 ± 0.01	10.65 ± 0.01	3.52 ± 0.01	113.0 ± 0.1	20 ± 3	0.152 ± 0.015	3.05 ± 0.12	>40,000	>39,940	Coarse-medium sand
Rapidan River														
RnR1-OSL1 BG5823 3.00	20/20	150-250	0.94 ± 0.03	14 ± 2	2.51 ± 0.01	6.94 ± 0.01	3.11 ± 0.01	92.2 ± 0.1	20 ± 3	0.152 ± 0.015	3.07 ± 0.09	290 ± 15	230 ± 15	Sand layer 20 cm above SSDs
RnR1-OSL2 BG5824 3.30	27/27	150-250	1.26 ± 0.04	18 ± 3	3.12 ± 0.01	9.49 ± 0.01	3.12 ± 0.01	84.9 ± 0.1	20 ± 3	0.147 ± 0.015	3.43 ± 0.10	355 ± 15	295 ± 15	Sand layer 10 cm below SSDs
RnR3-OSL1 BG5425 2.75	18/20	150-250	1.29 ± 0.04	13 ± 2	3.81 ± 0.01	13.80 ± 0.01	2.29 ± 0.01	134.5 ± 0.1	20 ± 3	0.156 ± 0.016	3.17 ± 0.09	390 ± 15	330 ± 15	Sand within interbedded silt & sand unit crosscut by dike
Rivanna River- Stigger Creek														
RR-SC2-OSL1 BG5820 3.05	19/20	150-250	41.60 ± 1.33	12 ± 3	3.37 ± 0.01	11.70 ± 0.01	2.77 ± 0.01	116.5 ± 0.1	20 ± 3	0.151 ± 0.015	3.44 ± 0.10	12,090 ± 525	12,030 ± 525	Reddish, silt; near dike tip
RR-SC2-OSL2 BG5821 3.30	20/20	150-250	68.69 ± 2.53	14 ± 3	3.12 ± 0.01	10.60 ± 0.01	2.72 ± 0.01	104.0 ± 0.1	20 ± 3	0.147 ± 0.015	3.13 ± 0.09	21,935 ± 1,005	21,875 ± 1,005	Mottled, silty sand; crosscut by dikes
RR-SC2-OSL3 BG5822 3.92	23/23	150-250	75.98 ± 2.79	14 ± 3	3.22 ± 0.01	11.50 ± 0.01	2.64 ± 0.01	106.0 ± 0.1	20 ± 3	0.138 ± 0.014	3.14 ± 0.07	24,200 ± 1,105	24,140 ± 1,105	Mottled, medium-fine sand; source layer of dikes

[a] Aliquots measured and used to define D_e population by Central Age or Minimum Age Model (Galbraith and Roberts, 2012).

[b] Equivalent dose calculated on a pure quartz fraction with ultra-small aliquots with 20-80 grains/aliquot and analyzed under blue-light excitation (470 ± 20 nm) by Single Aliquot Regeneration protocols (SAR; Murray & Wintle, 2003; Wintle & Murray, 2006). Equivalent dose (D_e) was calculated by Central Age or Minimum Age model when overdispersion values are < 20% (at two sigma) and >20% (at two sigma) and assuming a normal data distribution (Galbraith and Roberts, 2012; Liang and Forman, 2019).

[c] Overdispersion values reflects precision beyond instrumental errors; values of ≤ 20% (at 1 sigma limit) indicate low dispersion in equivalent dose values and defines a unimodal distribution. Values > 20% are associated with mixed equivalent dose signature reflecting multiple grain populations or partial solar resetting.

[d] U, Th, Rb and K content analyzed by inductively coupled plasma-mass spectrometry by ALS Laboratories, Reno, NV.

[e] Includes a cosmic dose rate calculated from parameters in Prescott and Hutton (1994) and includes soft components (Liang and Forman, 2019).

[f] Systematic and random errors calculated in a quadrature at one standard deviation by the Luminescence Dating and Age Calculator (LDAC) at https://www.baylor.edu/geosciences/index.php?id=962356 (Liang and Forman, 2019). Datum year is AD 2010. OSL ages determined at Geoluminescence Dating Research Laboratory, Dept. of Geosciences, Baylor University, Waco, TX, USA.

[g] Yr. B.P. = year before AD 1950.

Table B-4: Recalculated Optically-Stimulated Luminescence Dating of Quartz Grains from Sediment in the CVSZ

Site-Sample Lab No. Depth (m)	Aliquots[a]	Grain Size (µm)	Equivalent Dose (De) (Gy)[b]	Over-dispersion (%)[c]	U (ppm)[d]	Th (ppm)[d]	K2O (%)[d]	H20 (%)	Cosmic Dose Rate (mGray/yr)[e]	Dose Rate (mGray/yr)	OSL Age (Yr)[f]	OSL Age Yr. B.P.[g]	Sample Description
Appomattox River													
AR1-OSL1 BG5380 1.55	34/35	150-250	0.08 ± 0.01	52 ± 8	1.94 ± 0.01	5.27 ± 0.01	1.12 ± 0.01	20 ± 2	0.178 ± 0.018	1.58 ± 0.04	40 ± 5	-20 ± 5	Base of upper sandy unit
AR1-OSL2 BG5381 2.05	27/35	150-250	43.64 ± 2.76	23 ± 4	2.54 ± 0.01	7.56 ± 0.01	1.23 ± 0.01	20 ± 2	0.168 ± 0.017	1.89 ± 0.06	23,250 ± 1,525	23,190 ± 1,525	Base of lower mottled silt unit
AR3-OSL1 BG5382 0.62	34/35	150-250	6.23 ± 0.23	17 ± 2	1.84 ± 0.01	4.34 ± 0.01	1.52 ± 0.01	20 ± 2	0.208 ± 0.021	1.79 ± 0.05	235 ± 15	175 ± 15	Base of upper sandy unit
AR3-OSL2 BG5383 0.90	34/35	100-150	6.23 ± 0.23	7 ± 1	3.15 ± 0.01	7.44 ± 0.01	1.67 ± 0.01	20 ± 2	0.187 ± 0.019	2.34 ± 0.07	2,630 ± 130	2,570 ± 130	Lower mottled silt unit; below buried soil
AR3-OSL3 BG5384 2.55	35/35	150-250	>110	NA	3.14 ± 0.01	9.50 ± 0.01	1.64 ± 0.01	20 ± 2	0.159 ± 0.016	2.36 ± 0.07	>46,450	>46,390	Pebble lense within silt unit
AR4-OSL1 BG5415 2.91	13/13	150-250	>110	NA	2.03 ± 0.01	5.23 ± 0.01	1.69 ± 0.01	20 ± 2	0.153 ± 0.015	2.05 ± 0.06	>54,000	>53,940	Sand layer in interbedded silt & sand unit
AR5-OSL1 BG5422 2.91	35/35	100-150	54.91 ± 4.47	28 ± 4	2.24 ± 0.01	6.25 ± 0.01	1.72 ± 0.01	20 ± 2	0.153 ± 0.015	2.06 ± 0.06	26,585 ± 2,195	26,525 ± 2,195	From yellowish red, very fine sandy silt, micaceous; 10 cm AWL
AR7-OSL1 BG5419 2.91	30/35	150-250	54.88 ± 1.64	17 ± 2	2.65 ± 0.01	7.27 ± 0.01	1.68 ± 0.01	20 ± 2	0.153 ± 0.015	2.21 ± 0.06	24,710 ± 995	24,650 ± 995	From reddish, silty m-f sand with peb-bles; 10 cm AWL
AR8-OSL1 BG5409 1.45	35/35	150-250	6.18 ± 0.10	8 ± 1	2.88 ± 0.01	7.60 ± 0.01	1.68 ± 0.01	20 ± 2	0.179 ± 0.018	2.26 ± 0.07	2,715 ± 95	2,655 ± 95	Near base of upper unit of brownish, silty very fine sand
AR8-OSL2 BG5408 1.59	34/34	100-250	8.35 ± 0.14	9 ± 1	3.05 ± 0.01	7.30 ± 0.01	1.76 ± 0.01	20 ± 2	0.176 ± 0.018	2.33 ± 0.07	3,550 ± 125	3,490 ± 125	From reddish brown, very fine sandy silt below silt loam
AR8-OSL3 BG5410 2.39	36/36	100-250	49.66 ± 1.57	17 ± 2	2.00 ± 0.01	5.58 ± 0.01	1.80 ± 0.01	20 ± 2	0.162 ± 0.016	2.05 ± 0.06	24,140 ± 1,020	24,080 ± 1,020	From mottled, silty very fine sand of lower unit
James River													
JR1-OSL1 BG4000.B 3.42	30/35	100-150	0.63 ± 0.01	34 ± 5	1.99 ± 0.01	6.93 ± 0.01	1.52 ± 0.01	20 ± 3	0.139 ± 0.013	2.15 ± 0.06	290 ± 10	230 ± 10	From layer in which dike terminates

Site-Sample Lab No. Depth (m)	Aliquots[a]	Grain Size (µm)	Equivalent Dose (De) (Gy)[b]	Over-dispersion (%)[c]	U (ppm)[d]	Th (ppm)[d]	K2O (%)[d]	H20 (%)	Cosmic Dose Rate (mGray/yr)[e]	Dose Rate (mGray/yr)	OSL Age (Yr)[f]	OSL Age Yr. B.P.[g]	Sample Description
Pamunkey River													
PR2-OSL1 BG5411 3.08	35/35	150-250	19.86 ± 0.63	18 ± 2	2.92 ± 0.01	10.55 ± 0.01	1.73 ± 0.01	20 ± 2	0.143 ± 0.016	2.43 ± 0.07	8,135 ± 305	8,075 ± 305	Mottled sandy silt; level of dike tips
PR2-OSL2 BG5412 3.70	34/36	150-250	40.37 ± 1.25	16 ± 2	3.04 ± 0.01	10.05 ± 0.01	1.78 ± 0.01	20 ± 2	0.140 ± 0.014	2.46 ± 0.07	16,405 ± 675	16,345 ± 675	Silty sand near bottom of cutbank
PR100-OSL1 BG5418 3.33	37/40	150-250	4.81 ± 0.18	22 ± 3	2.72 ± 0.01	9.15 ± 0.01	1.74 ± 0.01	20 ± 2	0.146 ± 0.015	2.33 ± 0.07	2,050 ± 100	1,990 ± 100	Mottled sandy silt; level w/ lower dike tips & 20 cm below upper dike tip
PR201-OSL2 BG5414 1.0	34/35	250-500	19.36 ± 0.78	22 ± 3	3.00 ± 0.01	3.89 ± 0.01	0.86 ± 0.01	20 ± 2	0.185 ± 0.018	1.47 ± 0.05	13,125 ± 645	13,065 ± 645	Base of upper pebbly sand unit
PR201-OSL1 BG5413 1.6	27/35	100-150	47.19 ± 2.19	22 ± 3	7.70 ± 0.01	9.76 ± 0.01	1.45 ± 0.01	20 ± 2	0.181 ± 0.018	3.21 ± 0.07	14,650 ± 790	14,590 ± 790	Lower reddish silt unit
Rivanna River- Stigger Creek													
RR-SC1-OSL1 BG4002.B 4.0	33/35	100-150	36.40 ± 0.86	14 ± 2	3.13 ± 0.01	10.30 ± 0.01	2.37 ± 0.01	20 ± 3	0.138 ± 0.014	3.27 ± 0.09	11,070 ± 425	11,010 ± 425	From sandy source layer of dikes
South Anna River													
SoAR7-OSL1 BG4001.B 1.10	31/36	100-150	16.22 ± 0.32	10 ± 1	2.28 ± 0.01	5.92 ± 0.01	1.02 ± 0.01	20 ± 3	0.179 ± 0.018	1.79 ± 0.05	9,075 ± 310	9,015 ± 310	Mottled clayey silt, level with dike tip
SoAR10b-OSL1 BG5416 1.48	11/11	100-150	>150	NA	2.61 ± 0.01	9.85 ± 0.01	1.52 ± 0.01	20 ± 2	0.179 ± 0.018	2.28 ± 0.06	>64,900	>64,840	Upper silt unit; 3-28 cm below dike tips
SoAR10b-OSL2 BG5417 2.23	34/35	150-250	29.55 ± 0.70	39 ± 5	2.04 ± 0.01	11.40 ± 0.01	1.42 ± 0.01	20 ± 2	0.164 ± 0.016	2.12 ± 0.06	13,860 ± 530	13,800 ± 530	Lower mottled silt & sand unit; 98 cm below dike tips

See Table B-3 for footnotes.

APPENDIX C GEOTECHNICAL DATA

Table C-1: Borehole Locations of Geotechnical Data from the Virginia DOT

Location Name (Map ID) [1]	Latitude N (Dec. Degrees)	Longitude W (Dec. Degrees)	Location Description
Rivanna River 1 (A)	37.9186	78.2977	Rt. 600 bridge near Lake Monticello
So. Anna River 1 (B)	37.9383	77.9830	Rt. 699 bridge near Yanceyville
So. Anna River 2 (C)	37.7923	77.8307	Rt. 610 bridge near Holly Grove
So. Anna River 3 (D)	37.7576	77.7011	Rt. 611 bridge on Dunn Chapel Road
James River (E)	37.5768	77.6793	Rt. 288 bridge west of Richmond
Pamunkey River 1 (F)	37.7889	77.3699	Rt. 301 bridge near Hanover
Pamunkey River 2 (G)	37.7153	77.2892	Rt. 615 bridge east of Hanover
Pamunkey River 3 (H)	37.6857	77.1833	Rt. 360 bridge northeast of Richmond
Mattaponi River 1 (I)	38.0188	77.3773	Rt. 722 bridge near Milford
Mattaponi River 2 (J)	37.9422	77.3205	Rt. 654 bridge south of Bowling Green
Mattaponi River 3 (K)	37.7869	77.1038	Rt. 360 bridge near Aylett
Rappahannock River 1 (L)	38.2897	77.4497	Rt. 3 bridge near Fredericksburg
Rappahannock River 2 (M)	38.1763	77.1868	Rt. 301 bridge at Port Royal
Potomac River 1 (N)	38.3394	77.0591	Rt. 206 bridge over William Creek near Dahlgren
Potomac River 2 (O)	38.2727	76.9978	Rt. 205 bridge over Tide Mill Stream southeast of Dahlgren
Rapidan River (P)	38.3590	77.9730	Rt. 522 bridge near Raccoon Ford
Appomattox River 1 (Q)	37.3406	78.4715	Rt. 15 bridge northwest of Farmville
Appomattox River 2 (R)	37.4531	78.1494	Rt. 621 bridge on Brook Hill Road
Appomattox River 3 (S)	37.4845	77.9654	Rt. 609 bridge south of Macon
Nottoway River 1 (T)	36.9755	77.7705	Rt. 610 bridge southwest of McKenney
Nottoway River 2 (U)	36.9438	77.7283	Rt. 85 bridge south of McKenney
Nottoway River 3 (V)	36.8989	77.4003	Rt. 95 bridge south of Stoney Creek

[1] Map ID shown on Figure 3-1.

Table C-2: Geotechnical Data from Borehole Logs from the Virginia DOT

Location Name Borehole #	Map ID[1]	Depth (m)	Description of Susceptible Sediment	Blow Count[2]
Rivanna River 1 BH 6	A	7.1 9.4	cohesionless sand gray sand with some silt	5 5
So. Anna River 1 BH 31	B	4.0 5.0 7.0	yellow-brown silty sand, trace clay with fine to coarse gravel contains mica & thin roots, loose yellow-brown silty sand, trace clay with fine to coarse gravel contains mica and thin roots, very loose dark, yellow-brown silty sand, contains mica, v. loose	6 2 4
So. Anna River 2 BH 10	C	8.0 9.0 11.0	micaceous, fine, wet sand with organics micaceous, fine, wet sand with organics micaceous, fine, wet, fine sand with organics	6 11 9
So. Anna River 3 65544 BH 8 745431 BH 5 BH7 BH 10	D	2.7-3.6 2.9-4.0 2.1-3.8 2.3-2.7	gray, alluvial sand brown, micaceous sand grayish brown, micaceous sand gray, micaceous sand	14 7 18 16
James River BH 7	E	4.2 5.3 6.3	sand, dark brown, wet, loose to dense sand, dark brown, wet, loose to dense sand, dark brown, wet, loose to dense	6 10 4
Pamunkey River 1 BH 2	F	4.5 6.1 7.6 9.1	gray sand gray sand gray gravelly sand gray gravelly sand	1 5 8 18
Pamunkey River 2 BH 1	G	6.6 7.7 8.6	gray sand with black heavy minerals gray sand with black heavy minerals gray sand with black heavy minerals	4 4 4
Pamunkey River 3 BH 2	H	7.9 9.4 11	gray micaceous, sand, fine, medium & coarse grain, with organic matter same as above same as above	2 10 20
Mattaponi River 1 BH 1	I	1.8 3.4	sand, gray, fine grained, mottled with brown clay sand, dark gray, fine grained, with clay & shell fragments	15 11
Mattaponi River 2 BH 4	J	3.1 4.6	gray, fine, micaceous silty sand gray, fine, micaceous silty sand	3 8
Mattaponi River 3 BH 5	K	4.0 5.5	gray sand with organics	19 22
Rappahannock R. 1 BH 5	L	3.4 6.4	brown sand with some organics gray sand	5 7
Rappahannock R. 2 BH 40	M	3.1	tan and gray silty sand	7
Potomac River 1 BH 1	N	15.4	gray sand	9
Potomac River 2 BH 006	O	1.5 4.6	white to gray, silty very fine sand white to gray, fine sand, trace of silt	20 15
Rapidan River BH 5	P	3.1 3.4	light brown silty fine sand with medium gravel towards base	4 22

Location Name Borehole #	Map ID[1]	Depth (m)	Description of Susceptible Sediment	Blow Count[2]
Appomattox R. 1 BH 4	Q	3.0	Sand and gravelly sand	19
Appomattox R. 2 BH 1 BH 2	R	2.9-4.3 5.8 7.6	gray, fine to coarse, poorly graded sand, very loose gray fine to coarse, poorly graded sand, with silt, trace gravel, contains organic matter, very loose same as above except medium dense	0 2 22
Appomattox R. 3 BH R-8	S	2.4 4.3 5.6	gray & brown, silty fine sand, contains mica gray & brown, silty fine sand, contains mica gray & brown, silty fine sand, contains mica	3 2 4
Nottoway River 1 BH 4 BH 5	T	1.8 4.6 1.8 3.4	gray silty sand gray silty sand gray sand gray sand	1 4 1 25
Nottoway River 2 BH 6 BH 10	U	3.6 4.9	silty sand sand	15 17
Nottoway River 3 BH 4	V	4.9	dark gray fine-grained sand with moderate clay	6

[1] Map ID shown on Figure 3-1.

[2] Blow count (N) is the total number of blows required to drive a split spoon sampler 0.3 m using standard hammer (63.5 kg) dropping 0.76 m.

APPENDIX D RESULTS OF LIQUEFACTION POTENTIAL ANALYSIS

Table D- 1: Results of Liquefaction Potential Analysis for Local Scenario Earthquakes

Location Name	Map ID[1]	Distance[2] (km)	Results[3,4,5] (WT@ 1 m)	Results[3,4,5] (WT@ 3 m)
1. Scenario earthquake M 5.25				
Mattaponi River 2	J	10	L	N
Rappahannock River 1	L	10	L/N	N
Rappahannock River 2	M	10	N	–
Potomac River 1	N	10	N	N
Rapidan River	P	10	N	–
Appomattox River 2	R	10	L	L
Appomattox River 3	S	10	L	N
2. Scenario earthquake M 5.5				
Mattaponi River 2	J	10	L	L
Mattaponi River 3	K	10	N	N
Rappahannock River 1	L	10	L	L/N
Rappahannock River 2	M	10	L	N
Potomac River 1	N	10	L	L
Potomac River 2	O	10	N	N
Rapidan River	P	10	L	N
Appomattox River 2	R	10	L	L
Appomattox River 3	S	10	L	L
3. Scenario earthquake M 5.75				
Mattaponi River 3	K	10	L	L/N
Rappahannock River 2	M	10	–	L/N
Potomac River 2	0	10	N	N
Rapidan River	P	10	–	L

[1] Map ID shown on Figure 3-1.

[2] Distance between scenario earthquake considered and geotechnical site data used in the analysis.

[3] L = Liquefaction likely for 45% - 100% of the layers analyzed; L/N = marginal because liquefaction predicted for 24% - 44% of the layers analyzed; N = liquefaction not likely because liquefaction predicted for less than 24% of the layers analyzed.

[4] WT = water table; depth used in liquefaction potential analysis.

[5] – = Analysis not performed for this scenario earthquake at this water table depth.

Table D- 2: Results of Liquefaction Potential Analysis for Historical Scenario Earthquakes

Location Name	Map ID[1]	Distance [2] (km)	Results[3,4,5] (WT@1 m)
1. Scenario earthquake M 4.8			
James River	E	5	N
2. Scenario earthquake M 5.0			
James River	E	5	L/N
James River	E	10	N
Pamunkey River 1	F	14	L/N
Appomattox River 2	R	10	L
3. Scenario earthquake M 5.25			
Rapidan River	P	10	N
James River	E	5	L
James River	E	10	L/N
James River	E	15	N
Pamunkey River 1	F	10	L
Pamunkey River 1	F	14	L/N
Pamunkey River 2	G	10	N
Appomattox River 2	R	15	L
Appomattox River 2	R	20	N
Appomattox River 3	S	10	L
Appomattox River 3	S	15	N
4. Scenario earthquake M 5.5			
Rapidan River	P	10	L
James River	E	10	L
James River	E	15	L/N
James River	E	20	N
Pamunkey River 1	F	14	L
Pamunkey River 1	F	20	N
Pamunkey River 2	G	10	L
Appomattox River 2	R	20	L
Appomattox River 2	R	30	N
Appomattox River 3	S	15	L
5. Scenario earthquake M 5.75			
Rapidan River	P	20	N
James River	E	20	L/N
James River	E	30	N
Pamunkey River 1	F	20	L
Pamunkey River 1	F	30	L/N
Pamunkey River 2	G	30	N
Pamunkey River 3	H	38	N
Appomattox River 2	R	30	L
Appomattox River 2	R	55	N
Appomattox River 3	S	20	L
Appomattox River 3	S	30	N
6. Scenario earthquake M 6.0			
Rapidan River	P	20	L
James River	E	20	L
James River	E	30	L/N

Location Name	Map ID[1]	Distance [2] (km)	Results[3,4,5] (WT@1 m)
Pamunkey River 1	F	30	L
Pamunkey River 2	G	30	L
Pamunkey River 2	G	35	L
Appomattox River 3	S	30	L

See footnotes below Table D-1.

Table D-3: Results of Liquefaction Potential Analysis for Mineral Scenario Earthquakes

Location Name	Map ID[1]	Distance[2] (km)	Results[3,4,5] (WT@ 1 m)	Results[3,4,5] (WT@ 3 m)
1. Scenario earthquake M 5.25				
South Anna River 1	B	10	L	N
South Anna River 2	C	20	N	N
2. Scenario earthquake M 5.5				
South Anna River 1	B	10	–	L
South Anna River 2	C	20	N	N
3. Scenario earthquake M 5.75				
South Anna River 2	C	20	L	N
Rivanna River 1	A	30	N	N
4. Scenario earthquake M 6.0				
South Anna River 2	C	20	–	L
Rivanna River 1	A	30	L	N
Appomattox River 3	S	47	N	–
Appomattox River 2	R	53	N	N
Pamunkey River 1	F	55	N	N
5. Scenario earthquake M 6.25				
South Anna River 3	D	29	N	N
Rivanna River 1	A	30	–	L
Appomattox River 3	S	47	L/N	–
Appomattox River 2	R	53	L	N
Pamunkey River 1	F	55	L/N	N
Pamunkey River 2	G	65	N	N
6. Scenario earthquake M 6.5				
South Anna River 3	D	29	L	L
Appomattox River 3	S	47	L	L
Appomattox River 2	R	53	L	L
Pamunkey River 1	F	55	L	L/N
Mattaponi River 2	J	58	N	N
Rappahannock River 1	L	63	N	–
Pamunkey River 2	G	65	L	N
7. Scenario earthquake M 6.75				
Pamunkey River 1	F	55	–	L
Mattaponi River 2	J	58	L	N
Rappahannock River 1	L	63	L	N
Pamunkey River 2	G	65	–	L
Pamunkey River 3	H	74	L/N	L/N
8. Scenario earthquake M 7.0				
Mattaponi River 2	J	58	–	L
Rappahannock River 1	L	63	–	L
Pamunkey River 3	H	74	L	L
Mattaponi River 3	K	78	N	N
Potomac 1	N	94	N	N

See footnotes below Table D-1.

Table D-4: Results of Liquefaction Potential Analysis for Ashland Scenario Earthquakes

Site Name	Map ID[1]	Distance[2] (km)	Results[3,4,5] (WT@ 1 m)	Results[3,4,5] (WT@ 3 m)
1. Scenario earthquake M 5.25				
Pamunkey River 1	F	10	L	L/N
Pamunkey River 2	G	16	N	N
2. Scenario earthquake M 5.5				
Pamunkey River 1	F	10	–	L
Pamunkey River 2	G	16	L	L
Mattaponi River 2	J	18	L	N
Pamunkey River 3	H	26	N	N
3. Scenario earthquake M 5.75				
Mattaponi River 2	J	18	L	N
Pamunkey River 3	H	26	L/N	L/N
4. Scenario earthquake M 6.0				
Mattaponi River 2	J	18	–	L
South Anna River 3	D	24	N	N
Pamunkey River 3	H	26	L/N	L/N
South Anna River 2	C	35	N	N
South Anna River 1	B	45	N	N
5. Scenario earthquake M 6.25				
South Anna River 3	D	24	L	N
Pamunkey River 3	H	26	L	L
Mattaponi River 3	K	29	N	–
South Anna River 2	C	35	L	L
South Anna River 1	B	45	L	N
Rappahannock River 1	L	54	N	–
Appomattox River 3	S	58	N	–
Appomattox River 2	R	74	N	–
6. Scenario earthquake M 6.5				
Mattaponi River 3	K	29	L	N
Rappahannock River 1	L	54	L/N	N
South Anna River 3	D	24	–	L
South Anna River 1	B	45	–	L
Appomattox River 3	S	58	L	N
Appomattox River 2	R	74	L	N
Rivanna River 1	A	78	N	N
7. Scenario earthquake M 6.75				
Mattaponi River 3	K	29	–	L/N
Rappahannock River 1	L	54	L	L/N
Appomattox River 3	R	58	L	L
Potomac 1	N	68	N	–
Appomattox River 2	S	74	–	L
Rivanna River 1	A	78	L	L

See footnotes below Table D-1.

Table D-5: Results of Liquefaction Potential Analysis for Holly Grove Scenario Earthquakes

Site Name	Map ID[1]	Distance[2] (km)	Results[3,4,5] (WT@ 1 m)	Results[3,4,5] (WT@ 3 m)
1. Scenario earthquake M 6.0				
South Anna River 3	D	13	L	L
South Anna River 1	B	15	L	L
Appomattox River 3	S	36	L/N	N
Rivanna River 1	A	43	N	–
Appomattox River 2	R	47	N	N
Pamunkey River 2	G	48	N	–
2. Scenario earthquake M 6.25				
Appomattox River 3	S	36	L	L/N
Rivanna River 1	A	43	L	N
Appomattox River 2	R	47	L	L/N
Pamunkey River 2	G	48	L	N
Pamunkey River 3	H	58	N	N
Mattaponi River 2	J	48	N	N
3. Scenario earthquake M 6.5				
Appomattox River 3	S	36	–	L
Rivanna River 1	A	43	–	L
Appomattox River 2	R	47	L	L
Pamunkey River 2	G	48	–	L
Pamunkey River 3	H	58	L/N	L/N
Mattaponi River 2	J	48	L	N
Mattaponi River 3	K	64	N	–
Rappahannock River 1	L	64	N	–
7. Scenario earthquake M 6.75				
Mattaponi River 2	J	48	L	L
Pamunkey River 3	H	58	L	L/N
Mattaponi River 3	K	64	N	–
Rappahannock River 1	L	64	L	L/N
Potomac 1	N	91	N	–

See footnotes below Table D-1.

Table D-6: Results of Liquefaction Potential Analysis for Wyndham Forest Scenario Earthquakes

Location Name	Map ID[1]	Distance[2] (km)	Results[3,4,5] (WT@ 1 m)	Results[3,4,5] (WT@ 3 m)
1. Scenario earthquake M 5.75				
Pamunkey River 1	F	21	L	L/N
Pamunkey River 2	G	25	L	N
South Anna River 2	C	26	N	N
2. Scenario earthquake M 6.0				
Pamunkey River 1	F	21	-	L
Pamunkey River 2	G	25	-	L
South Anna River 2	C	26	L	L/N
Pamunkey River 3	H	34	L/N	-
Mattaponi River 2	J	35	N	-
3. Scenario earthquake M 6.25				
South Anna River 2	C	26	-	L
Pamunkey River 3	H	34	L/N	L/N
Mattaponi River 2	J	35	L	N
Mattaponi River 3	K	42	N	-
Appomattox River 3	S	42	L	N
Appomattox River 2	R	58	L	N
South Anna River 1	B	46	L	N
4. Scenario earthquake M 6.5				
Pamunkey River 3	H	34	L	L
Mattaponi River 2	J	35	-	L
Mattaponi River 3	K	42	N	-
Appomattox River 3	S	42	L	L
South Anna River 1	B	46	L	L
Appomattox River 2	R	58	-	L
Rivanna River 1	A	69	N	-
Nottoway River 1	T	82	N	-
5. Scenario earthquake M 6.75				
Mattaponi River 3	K	42	N	N
Rivanna River 1	A	69	L	L
Nottoway River 1	T	82	L/N	-
Appomattox River 1	Q	89	N	-
Nottoway River 3	V	90	N	-
6. Scenario earthquake M 7.0				
Mattaponi River 3	K	42	N	N
Nottoway River 1	T	82	L	N
Nottoway River 2	U	85	N	-
Nottoway River 3	V	90	L	N

See footnotes below Table D-1.

Table D-7: Results of Liquefaction Potential Analysis for Macon Scenario Earthquakes

Location	Map ID[1]	Distance[2] (km)	Results[3,4,5] (WT@ 1 m)	Results[3,4,5] (WT@ 3 m)
1. Scenario earthquake M 5.5				
Appomattox River 3	S	5	L	L
Appomattox River 2	R	21	L	N
2. Scenario earthquake M 5.75				
Appomattox River 2	R	21	-	L
3. Scenario earthquake M 6.0				
South Anna River 2	C	35	N	-
4. Scenario earthquake M 6.25				
South Anna River 2	C	35	L	L/N
South Anna River 3	D	35	N	-
South Anna River 1	B	51	N	-
Nottoway River 1	T	56	N	-
Pamunkey River 1	F	58	N/L	N
5. Scenario earthquake M 6.5				
South Anna River 2	C	35	-	L
South Anna River 3	D	35	L	N
South Anna River 1	B	51	L	L/N
Nottoway River 1	T	56	L/N	L/N
Pamunkey River 1	F	58	L	L/N
Rivanna River	A	59	L	N
Pamunkey River 2	G	61	L	N
6. Scenario earthquake M 6.75				
South Anna River 3	D	35	-	L
Nottoway River 1	T	56	L	L/N
Pamunkey River 1	F	58	-	L
Rivanna River	A	59	-	L
Pamunkey River 2	G	61	-	L
Pamunkey River 3	H	68	L/N	L/N
Mattaponi River 2	J	73	L	N
Nottoway River 3	V	80	N	-
7. Scenario earthquake M 7.0				
Appomattox River 1	Q	52	N	-
Nottoway River 1	T	56	-	L
Nottoway River 2	U	62	N	-
Pamunkey River 3	H	68	L	L
Mattaponi River 2	J	73	-	L
Mattaponi River 3	K	79	N	-
Nottoway River 3	V	80	L	N

See footnotes below Table D-1.